INFORMATION TO USERS

This manuscript has been reproduced from the microfilm master. UMI films the text directly from the original or copy submitted. Thus, some thesis and dissertation copies are in typewriter face, while others may be from any type of computer printer.

The quality of this reproduction is dependent upon the quality of the copy submitted. Broken or indistinct print, colored or poor quality illustrations and photographs, print bleedthrough, substandard margins, and improper alignment can adversely affect reproduction.

In the unlikely event that the author did not send UMI a complete manuscript and there are missing pages, these will be noted. Also, if unauthorized copyright material had to be removed, a note will indicate the deletion.

Oversize materials (e.g., maps, drawings, charts) are reproduced by sectioning the original, beginning at the upper left-hand corner and continuing from left to right in equal sections with small overlaps.

Photographs included in the original manuscript have been reproduced xerographically in this copy. Higher quality 6" x 9" black and white photographic prints are available for any photographs or illustrations appearing in this copy for an additional charge. Contact UMI directly to order.

ProQuest Information and Learning
300 North Zeeb Road, Ann Arbor, MI 48106-1346 USA
800-521-0600

UNIVERSITY OF ALBERTA

A functional dissection of the *vestigial* gene

BY

Julie Olivia MacKay 

A thesis submitted to the Faculty of Graduate Studies and Research in partial fulfillment of the requirements for the degree of Master of Science

IN

MOLECULAR BIOLOGY AND GENETICS

DEPARTMENT OF BIOLOGICAL SCIENCES

Edmonton, Alberta
Spring, 2001

UNIVERSITY OF ALBERTA
LIBRARY RELEASE FORM

NAME OF AUTHOR: Julie Olivia MacKay

TITLE OF THESIS: A functional dissection of the *vestigial* gene

DEGREE: Master of Science

YEAR THIS DEGREE GRANTED: 2001

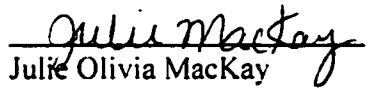

Julie Olivia MacKay
904 36 St. NW
Calgary, AB
T2N 3A8

Dec 15, 2000

UNIVERSITY OF ALBERTA

FACULTY OF GRADUATE STUDIES AND RESEARCH

The undersigned certify that they have read, and recommended to the Faculty of Graduate Studies and Research for acceptance, a thesis entitled "A functional dissection of the *vestigial* gene" submitted by Julie Olivia MacKay in partial fulfillment of the requirements for the degree of Master of Science in Molecular Biology and Genetics.

Dr. John Bell

Dr. Ross Hodgetts

Dr. Shelagh Campbell

Dr. Michael Walter

Table of Contents

List of Figures

Tables

Abstract

The genes *vestigial* and *scalloped* are implemented for important roles during the formation of the *Drosophila* wing. They act cooperatively to achieve coordination and regulation of wing development. Several recent studies have unfolded the physical and synergistic interaction between these two genes. The exact domain in Vg that interacts with Sd has been identified and localized to a 56 amino acid region, namely amino acids 279-335 of the vg ORF. Sd is required for the nuclear localizaion and hence proper action of the nuclear Vg protein. The human homologue of Sd, TEF-1, is a transcriptional enhancing factor that is able to substitute for Sd. The hypothesis that a Vg/Sd heterodimer acts as a complex to exert a transcriptional activation role seems plausible.

This study performs a functional dissection of the *vg* ORF. to determine the necessary elements for *vg* to properly carry out its role . The UAS-Gal4 system was utilized to address this question in two ways. Firstly, several deletions of the *vg* ORF were constructed and used to examine which regions were required for the ectopic induction of Sd expression. Secondly. the same deletions were used to examine their ability to rescue two *vg* mutants, vg^{83b27} and vg^{1}.

Both assays were successful in determining the presence of two activation domains in Vg, contained in residues 1-170 and 335-453. This correlates well with yeast one hybrid studies (Vaudin et al., 1999) which identified two activation domains in Vg located in amino acids 7-127 and 357-453. The authenticity of these domains and the role of Vg as a transcriptional activator are supported by these findings.

Acknowledgements

This work was supported by the Natural Sciences and Engineering Research Council (NSERC) of Canada, granted to Dr. John Bell. I would like to acknowledge Andrew Simmonds for deletion constructs used in this work and technical advice. Thank you to Iga Stepcynski for being a good friend and surviving 207 with me. Thanks to Sandra O'keefe for technical advice and conversations at lunch. A special thanks to John for allowing me to learn as I went along in my project and for leisure Fridays. A big thank you to Kelly Soanes for being a very patient teacher in the lab and always being very supportive (buddy!). To Mom, Dad and everyone at home in Nova Scotia, you're far away, but the support still gets here...thank you!

Introduction

Extensive knowledge has been gathered on segmental patterning, embryo and adult body patterning, appendage formation and developmental regulation in *Drosophila*. The use of a limited number of pathways in different tissues which result in the production of different cell fates has become a common theme in many studies in *Drosophila* and other organisms. Repetition of signaling and receptor molecules makes it essential that specificity of target and signaling molecules be conferred at a certain time, space and area in developing tissues. To examine these intricate relationships and organization of developing tissue, I will focus on wing development in *Drosophila* and the specificity of its formation, with emphasis on the *vestigial* (*vg*) and *scalloped* (*sd*) genes.

Pattern formation

In early studies of pattern formation, clonal analysis was used (Crick and Lawrence, 1975; Garcia-Bellido et al.,1976) to assess the developmental capacity of individual cells. This process is still used today and laid the groundwork for the ongoing work of understanding the formation and maintenance of compartments and borders within developing tissues.

Deciphering the mysteries of pattern formation has been the interest of many researchers in many different fields and branches of developmental biology. The focus of these early works was the investigation of how developing tissues are organized and follow such strict rules of formation. In 1976 the polar coordinate system (French et al.,

1976) was proposed to explain how the fields within these tissues were organized. They defined fields as 'domains within which changes in the presumptive fates of cells (regulation) can occur in response to surgical manipulation' and as 'a set of cells which have their positions specified with respect to the same coordinate system' (French et al., 1976). The coordinates that were assigned to different parts of developing tissues were used to explain how regeneration or duplication events occurred in response to removal or transplantation of specific areas of tissue. This approach was intended to examine if the rules that individual cells obeyed, with respect to their behavior, could explain the behavior of their respective tissues. This model worked to some extent, but the biochemical and molecular basis for these decisions was a much-needed key to explain the specification of different domains.

Pattern formation refers to the process which leads to a predictable spatial pattern of differentiation within developing tissue (Ashburner and Wright, 1978). Within the developing fly there are many processes which need to be followed to complete this predictable pattern to obtain the desired outcome--the adult fly. The spatial and temporal patterns that are organized in the developing fly follow a complicated but required path. To understand how pattern formation occurs successfully in the fly, one must understand the steps involved at each level of development that together ultimately construct the adult fly.

Embryonic patterning involves a cascade of inter-related genes, each responsible for ensuring the embryo is divided up appropriately to bestow correct identity to each region. The maternal effect genes are responsible for organizing the initial global alterations within the embryo. For example, *bicaudal* is expressed in the posterior half of

the embryo (Nusslein-Volhard and Weischaus, 1980). Throughout the ontogeny of the developing fly, the families of genes mentioned below are sequentially activated.

The differential response that zygotic genes have to the initial maternal gradients results in further subdivision and specification of the embryo into segments. Gap gene expression results in specification of position along the A-P axis of the embryo. These positions are defined by unique values and are required for proper segmental subdivision and consequently one continuous body region. This group includes such genes as *Krüppel*, *hunchback* and *knirps* (Nusslein-Volhard and Weischaus, 1980).

Next in this cascade are the pair-rule genes. When these genes are mutated, homologous parts of the pattern are deleted in every other segment. This observation by Nusslein- Volhard and Weischaus (1980) was the first hint at the existence of parasegment-like organization in the embryo. This group includes genes such as *even-skipped*, *odd-skipped*, *paired*, *runt*, and *hairy* (Nusslein-Volhard and Weischaus, 1980).

The segment polarity genes are next to respond, and mutants of these genes show deletions within each body segment. The remaining portion undergoes a mirror image duplication. Thus, the segment polarity genes are necessary to establish the first basic pattern of the segmental units in the fly. Some of the genes in this category include, *fused*, *wingless*,*engrailed*, *cubitus interruptus*, *gooseberry*, *hedgehog* and *patch*, and are zygotic embryonic lethals when mutated (Nusslein-Volhard and Weischaus, 1980).

The final members of this temporal cascade are the homeotic genes, which play a very important role in specifying parasegment character. Mutants in this class show a transformation from one segment type to another. Within this class, *Antennapedia* (ANT-C) and *bithorax* (BX-C) expression overlap to create very strict regions. Throughout the

cascade, the set of genes preceding another defines in some manner where and when the next genes will act (**Figure 1**, Ingham, 1988).

Imaginal discs

Whenever studying aspects of developmental patterning of the fly one should keep in mind the striking similarities between the larval and adult structures. The imaginal discs, which are all paired except for the genital disc, correspond to adult structures in a similar spatial arrangement. They provide very useful tools to use in patterning studies and offer several benefits, including (1) making use of genetic mutations, (2) there is a complete temporal distinction between when the presumptive pattern is formed and when it is realized during differentiation, and (3) the complexity of the patterns within the developing discs offers scientists a clear understanding of the individual parts of the discs and allows them to be followed with precise markers (Asburner and Wright, 1978). The determination of a particular cell fate and the heritable commitment of that fate are precisely linked.

For the interest of the work presented herein, the patterning of the wing imaginal disc is of great importance. The wing and lateral half of the notum is produced by each wing disc, as well as several pleural plates located on the lateral surface of the mesothorax. The wing disc has been, and still is being, dissected to understand what is working where and when in this developing tissue. The wing disc fate map (**Figure 2**) shows the general pattern of the wing disc with respect to the presumptive tissues each region will give rise to (Bryant, 1975). The corresponding structures in the adult fly (**Figure 3**) can be traced back to this original organization.

Figure 1. Patterning of the developing embryo in *Drosophila*. Expression of maternal, gap, pair rule and homeotic genes leads to the formation of the segmented embryo. The early embryo is divided by maternal gradients established by *bicoid (bcd)* in the anterior pole and *nanos (nos)* in the posterior pole. Gap genes are zygotically transcribed in broad domains (*hunchback, hb and Kruppel, Kr*). Maternal *hb* is already present in the anterior half of the egg. The pair-rule genes *hairy (h)* and *runt* require the activity of gap genes and begin to narrow their respective domains into striped patterns. Homeotic genes are expressed in regions specified by gap gene activity. Eventually the parasegmented embryo is achieved. Taken from Ingham., 1988.

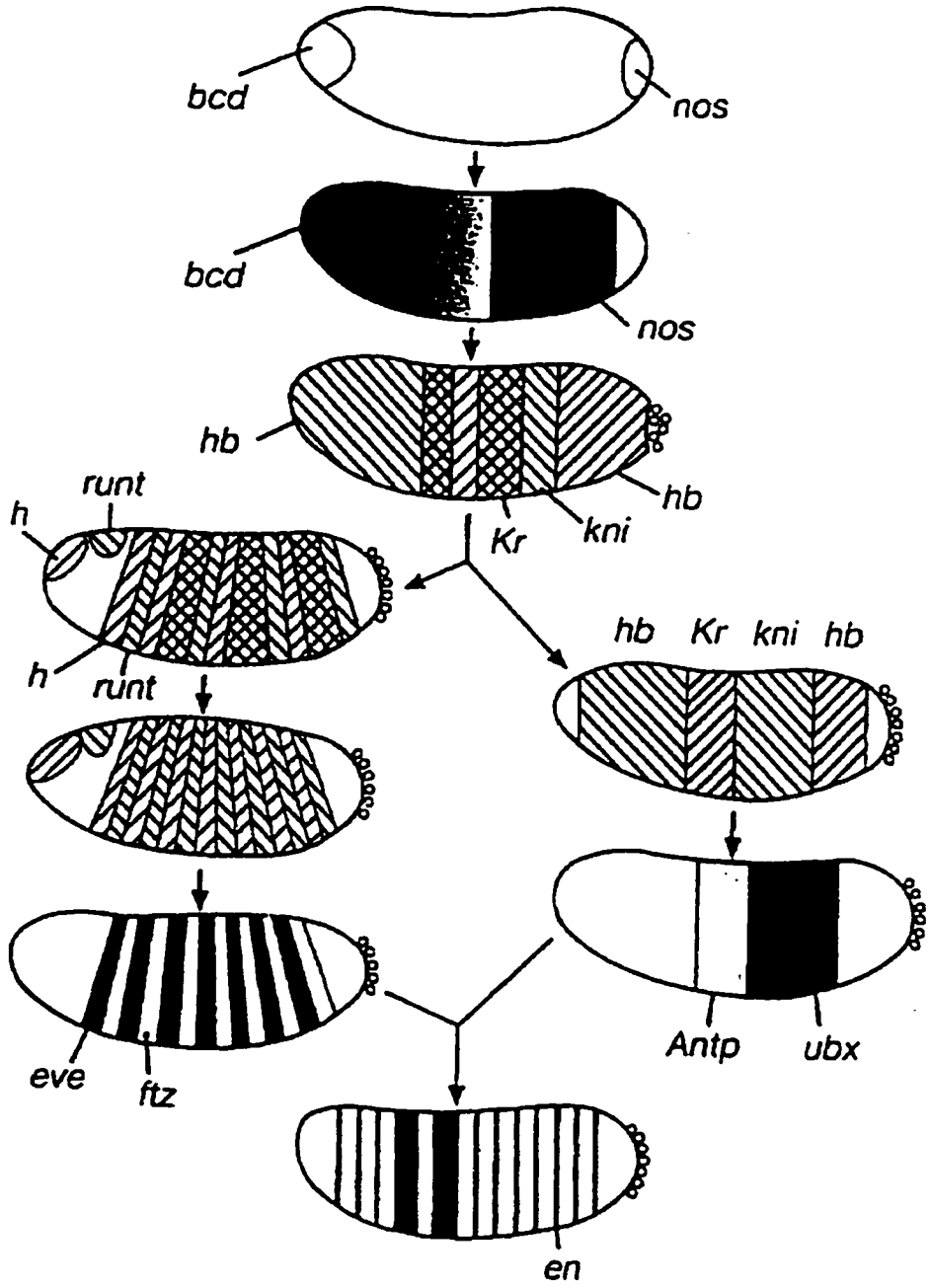
bcd
nos
bcd
nos
hb
hb
kni
Kr
runt
h
h
runt
hb Kr kni hb
eve
ftz
Antp
ubx
en

Figure 2. The wing disc fate map (Bryant, 1975). The wing disc can be dissected to compare which regions correspond to the ultimate adult structures. Wing and notum are divided into regions fated to become adult structures (see legend provided).

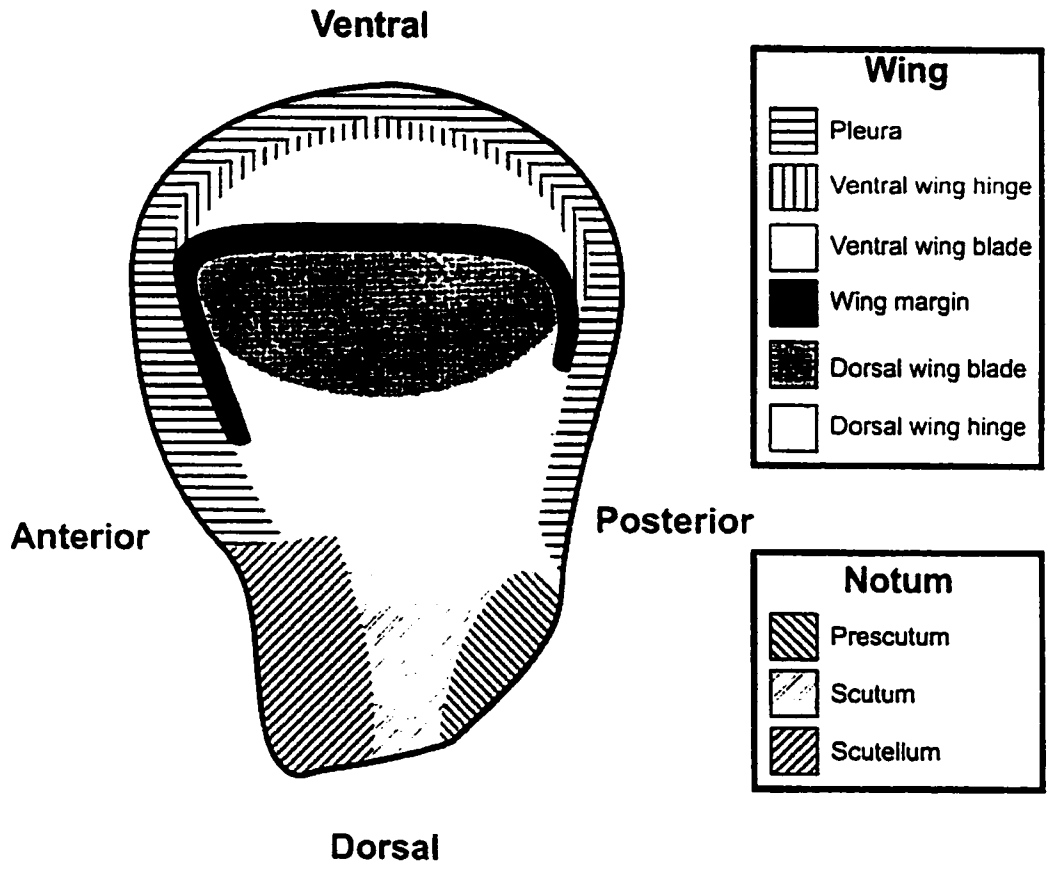
Ventral
Anterior
Posterior
Dorsal
Wing
Pleura
Ventral wing hinge
Ventral wing blade
Wing margin
Dorsal wing blade
Dorsal wing hinge
Notum
Prescutum
Scutum
Scutellum

Figure 3. Diagrams of adult dorsal **(A)** and ventral **(B)** wing structures and hinge (adopted from Bryant, 1975). Abbreviations are as follows: Ps, prescutum; Sc, scutum; Scl, scutellum; TR, triple bristle row (anterior wing margin); DR, double bristle row (distal wing margin); PR, posterior row of hairs; cs, capaniform sinsillae; MP, mesopleura; PtP, pteropleura; PP, postpleura; PN, postnotum.

A

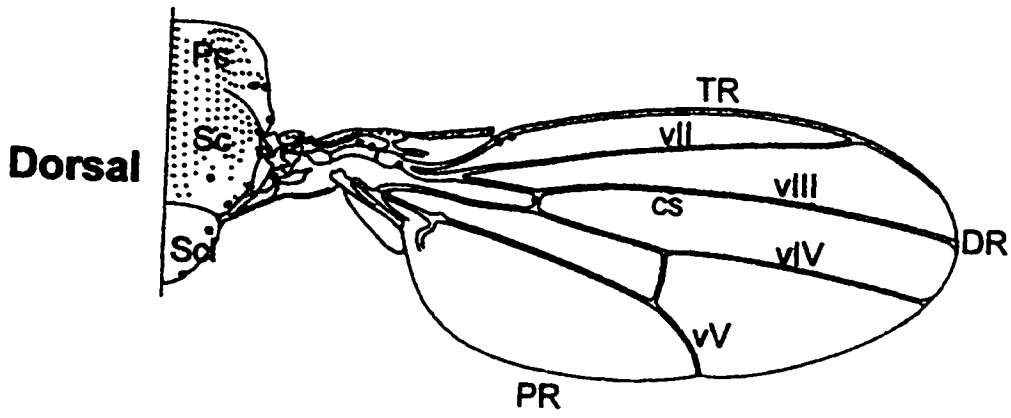
Dorsal
Pt
Sc
Sc'
TR
vII
vIII
cs
vIV
vV
DR
PR

B

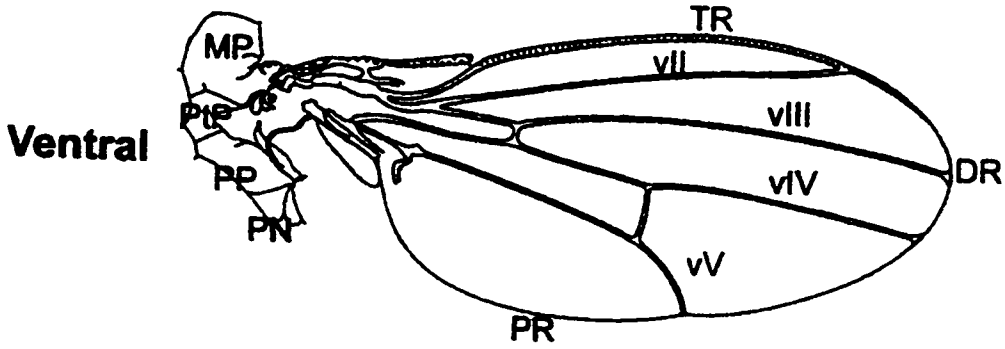
Ventral
MP
Pt'
cs'
PP
PN
TR
vII
vIII
vIV
vV
DR
PR

Drosophila wings are organized via long and short-range signals that establish polarity and proper tissue formation (Neumann and Cohen, 1997). The *dpp* gene product is produced along the anteroposterior (A/P) border of the wing imaginal disc and induces other wing specific genes, including *spalt*, *spalt-related* and *optomtor blind*, along the center of the *dpp* expression pattern. The *wg* pathway specifies the dorsoventral (D/V) boundary in the developing disc. *wg* promotes specific expression of *apterous* (*ap*) in the dorsal compartment, and *serrate* in the ventral compartment (Williams et al., 1993). Together, the *dpp* and *wg* pathways act to broadly divide the disc into A/P and D/V compartments (Neumann and Cohen, 1997).

wing specific organizers

One of the genes involved in wing development, *vestigial*, was first identified in 1911 by Morgan. The phenotypes of *vestigial* mutants vary in severity. Examples are shown in **Figure 4**, where defects in the wing range from smaller, crumpled wings to complete ablation of wings. Much information has been gathered on *vestigial* and how it works to promote proper wing development in the fly. The *vestigial* gene product is in fact present in a number of developing tissues (see Williams et al., 1991), but particularly in the wing and haltere imaginal discs (Stanley, 1931; Fristrom, 1969; Bownes and Roberts, 1981). Vg expression has been used as the earliest specific marker for wing primordia (Williams et al., 1991). The wing defects, described previously, are due to an increase in cell death in third larval instar imaginal discs (Fristrom, 1969; Bownes and Roberts, 1981). In the wing imaginal discs, specifically, anti-*vg* antibody stains the portion of the discs fated to become the wing and hinge surface in the adults, and

Figure 4. Various degrees of severity seen in *vestigial* mutants are illustrated. Wild-type wings are shown in class I, and classes II-X are representative of the varying degrees of phenotypes seen in *vg* mutant flies (Nakashima-Tanaka, 1967).

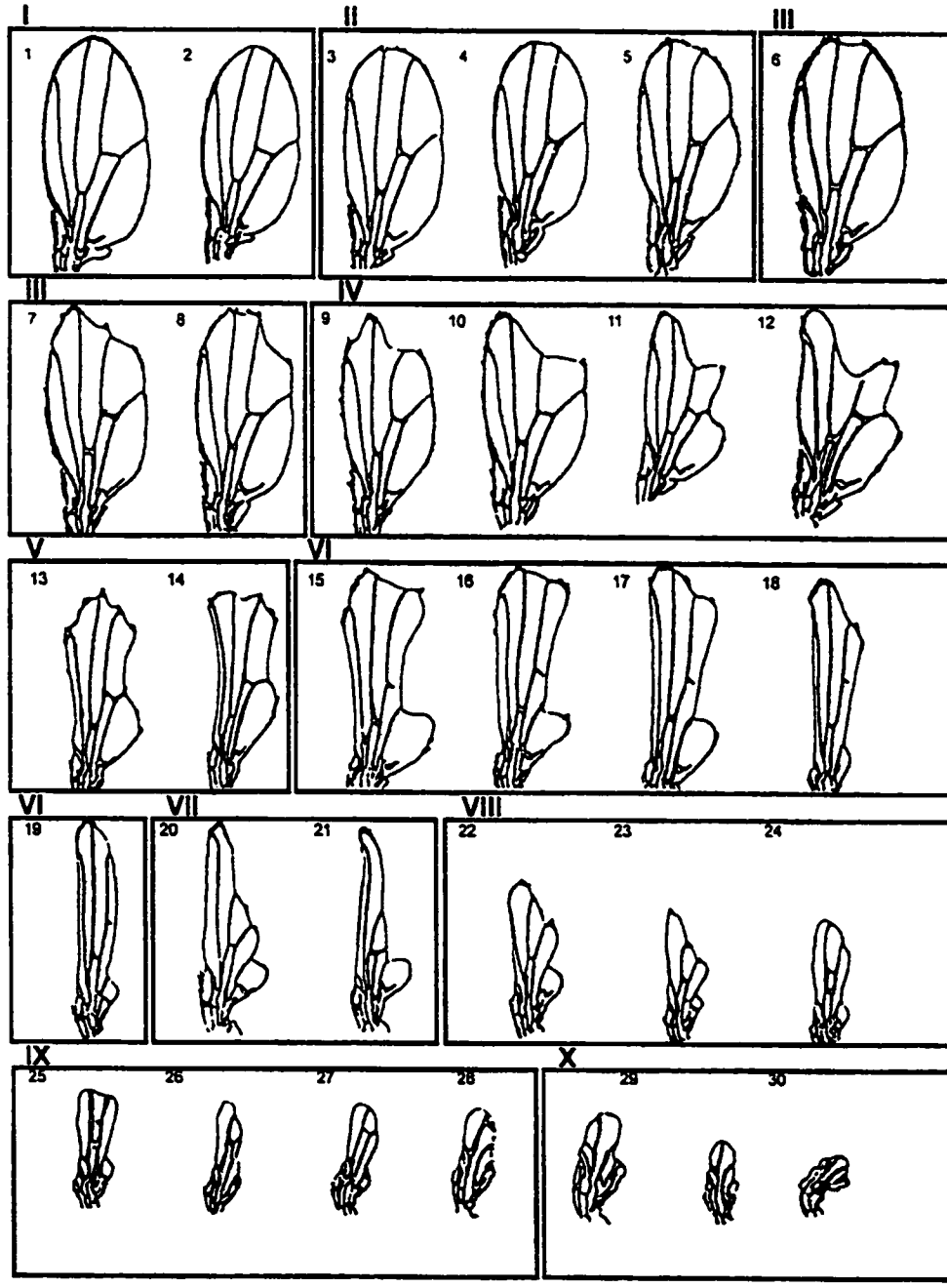
I
1
2
II
3
4
5
III
6
III
7
8
IV
9
10
11
12
V
13
14
VI
15
16
17
18
VI
19
VII
20
21
VIII
22
23
24
IX
25
26
27
28
X
29
30

overlapping anti-*vg* and anti-*ap* antibody define the dorsal surface of the wing (Williams et al., 1993).

vg is a target of both the *dpp* and *wg* pathways and is involved in proper wing development. *vg* expression occurs throughout the entire wing field (Williams et al., 1991, 1993; Kim et al., 1996), as shown in Figure 6a,b, Williams et al. (1991). Two different *vg* enhancers act to organize the wing imaginal disc and guide, by promoting or restricting, *vg* expression. These enhancers, called the boundary and quadrant enhancers, are induced by two different signaling pathways. The boundary enhancer (*vg*BE) acts along the D/V border and is mediated by the *ap-fng-Ser-Notch* pathway and *Suppressor of hairless* (*Su(H)*) (Williams et al., 1994; Kim et al., 1996). The *vg*BE expression covers a thin stripe in the prospective wing margin (Figure 6 in Klein and Arias, 1999). The quadrant enhancer (*vg*QE) coordinates *vg* expression in the rest of the wing pouch and requires D/V organizer activity to function properly. Activation of the quadrant enhancer is accomplished by the *dpp* and *wg* inducers (Kim et al., 1996; Neuman and Cohen, 1997). The *vg*QE acts later in development in all four quadrants of the wing disc, complementing the *vg*BE and filling in the developing wing blade (Klein et al., 1999). The *vg*BE is localized within intron 2 of *vg* and interacts with the *vg*QE, which is contained in intron 4 (**Figure 5**).

The expression pattern of *vg* in the wing disc varies among *vg* mutants. For example, the recessive null *vg* mutant, vg^{83b27} (**Figure 6 A**) is due to loss of the *vg*BE. Thus, *vg* is not induced and wings are absent. The weaker *vg* null, vg^{1} (**Figure 6 B**) has reduced wing tissue. Ectopic expression assays with *vg* (Halder et al., 1998) have shown

Figure 5. Locations of *vg*QE and *vg*BE. The boundary and quadrant enhancers in introns 2 and 4, respectively, of the *vg* gene are activated by the *N-Su(H)* and *dpp* pathways. Activation of the QE (blue box) occurs via unknown signal(s) from the BE (XX) and Dpp signaling, from the A/P boundary. The BE (yellow box) is directly activated by the N-Su(H) pathway at the D/V boundary. Bars represent exons, while shaded black bars represent expressed portion of the exons and lines represent introns (identified by their respective number). The resulting expression of each enhancer in the wing disc is shown below the schematic, where the *vg*BE is shown in yellow and the *vg*QE in light blue. Taken from Kim et al., 1996.

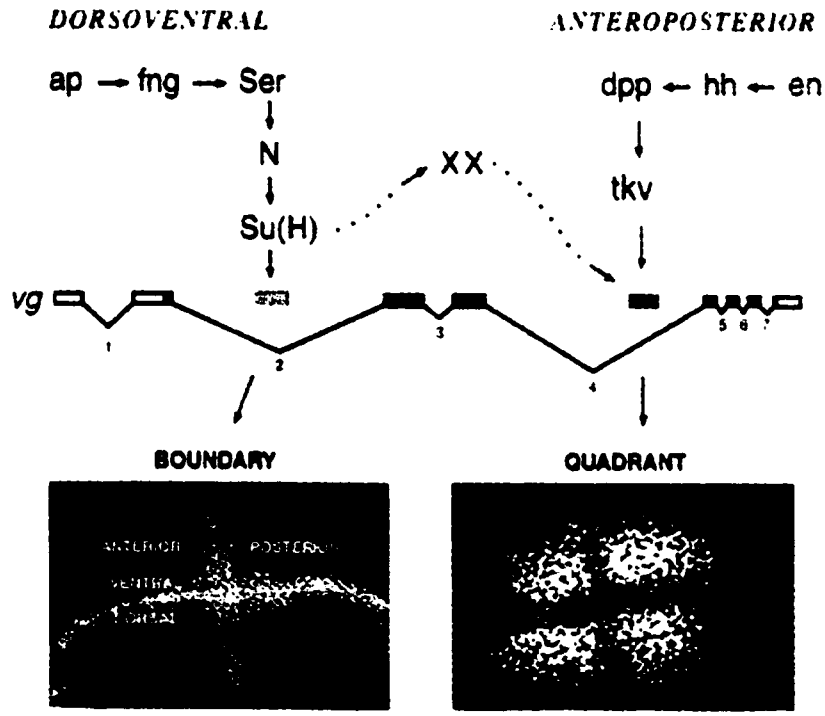
DORSOVENTRAL
ANTEROPOSTERIOR
ap → fng → Ser
N
Su(H)
XX
dpp ← hh ← en
tkv
vg
1
2
3
4
5 6 7
BOUNDARY
QUADRANT

Figure 6. The phenotypes of vg^{83b27} **(A)** and vg^{1} **(B)**. The vg^{83b27} , mutant, due to a 3 kb deletion, including the vg BE (Williams et al. 1990), has only partial hinge tissue compared to the less severe vg^{1} mutant, which is the result of a 8kb 412 transposon insertion in intron 3 (Williams et al., 1991).

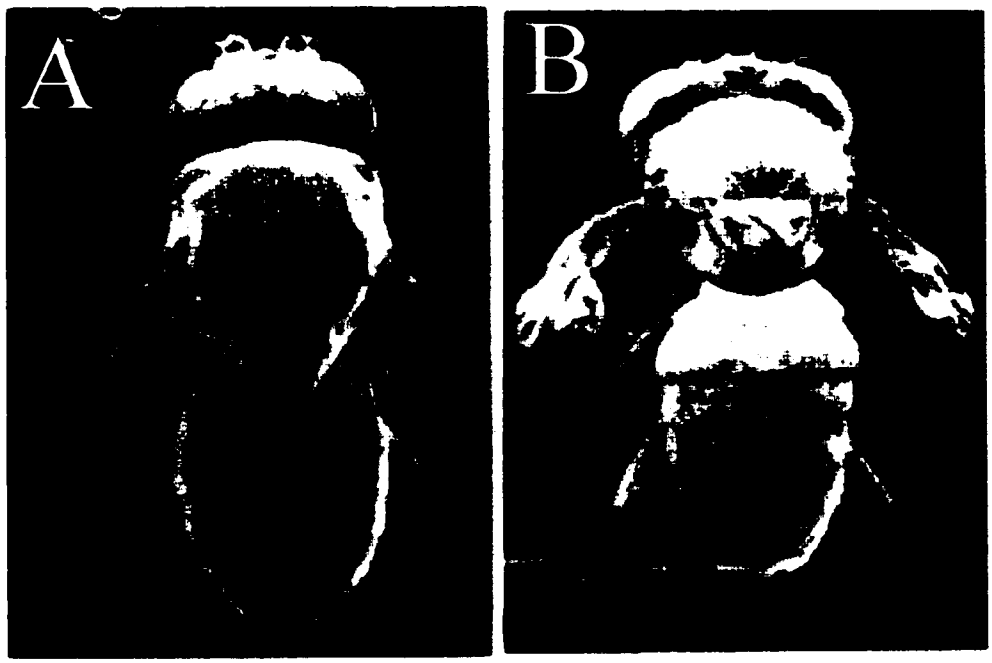
A
B

that *vg* exhibits selector gene characteristics; it is able to re-program cells to adopt a wing-like fate. From the normal expression pattern as well as from ectopic expression results, it seems as though *vg* is specifically involved and required for wing development. However, its mode of action is only recently being unraveled.

vg has been shown to interact with another important wing gene, scalloped (*sd*). The expression pattern of *sd* in the wing imaginal disc (Williams et al., 1991, 1993; Campbell et al., 1992) is almost identical to that of *vg* (Figure 5 A and B respectively, Williams et al., 1993). However, *sd* is more widely expressed in other developing tissues compared to the more constricted expression of *vg*, specifically in the wing disc. Some *sd* mutants may result in phenotypes similar to *vg* mutants (Campbell et al., 1992), although other *sd* mutants are lethals as homozygotes. Most viable *sd* mutants show ectopic sensory bristles, as well as wing margin defects including minor nicks to complete ablation and reduced wing blade surface (Figure 4, Campbell et al., 1992). Characterization of *sd* (Campbell et al., 1991, 1992) has identified it as a gene encoding a DNA binding protein that belongs to the TEA family.

The human homologue of *sd*, transcriptional enhancing factor-1 (TEF-1) (Jacquemin et al., 1996), is able in *Drosophila* to substitute for Sd for proper Vg function (Deshpande et al., 1997) and binds Vg with the same ability as Sd (Simmonds et al., 1998). The TEF-1 protein binds cooperatively to tandem repeats of the GT-IIC or Sph enhansons of the human Simian virus 40 enhancer and promotes viral DNA replication and replication-independent activation of transcription (Kelly and Wildeman, 1991). TEF-1 has the ability to activate or repress promoter activity, which is governed by the limiting presence of transcription intermediary factor (TIF) (Xiao et al., 1991). Indeed, it

has been proposed that Vg serves as the *Drosophila* TIF for Sd in the developing wing (Simmonds et al., 1998). This functional homology of Sd with TEF-1 provides opportunity for *Drosophila*/human comparisons. Overlapping expression patterns of Sd and Vg, and protein-protein interactions all support the idea that Vg and Sd interact physically and in parallel to properly form the wing. Halder et al. (1998) used *vg*Gal4 assays to show that up-regulated *sd* occurred wherever *vg* was able to successfully induce ectopic wing structures. As well, when *vg* was expressed in the absence of Sd, Vg was detected in the cytoplasm and nuclei. In contrast, when Sd is present Vg is localized solely to the nucleus. In *sd* mutants, the ability of *vg* to ectopically induce wing tissue is greatly reduced or non-existent. Physical interaction between Sd and Vg was also shown to occur (Simmonds et al., 1998). *In vitro*-binding experiments showed that the protein-protein interaction between Sd and Vg is specifically confined to a 56 amino acid region in the *vg* protein, between residues 279 and 335. Thus, it appears that Sd and Vg act together as a transcriptional activator during wing formation, wherein Sd provides the DNA binding activity and nuclear localization and Vg provides the activation domain.

Many of the same pathways are used for regulating and inducing several different genes in the same tissue. Thus, how is it that the different *vg* enhancers are activated exclusively in a particular area by the same signal? It would seem reasonable that there are other counterparts or processes that enable these genes to be able to respond specifically to these signals at the right time and place. The selector and signal model (Halder et al., 1998) (**Figure 7**) suggests that three different signaling proteins (blue) are acting in combination to control target gene responses of wing specific-genes (red). The

Figure 7. The selector and signal model proposed modified from Halder et al.. 1998. Signaling proteins (Hh, Ser, dpp; grey) act to control wing-specific gene targets (SRF-A, *vg* boundary and *vg* quadrant enhancers; red). The expression of these targets is restricted to the wing pouch via Vg/Sd control (green) and display different patterns due to the regulation by Ci, Su(H) and Mad proteins (shown in blue).

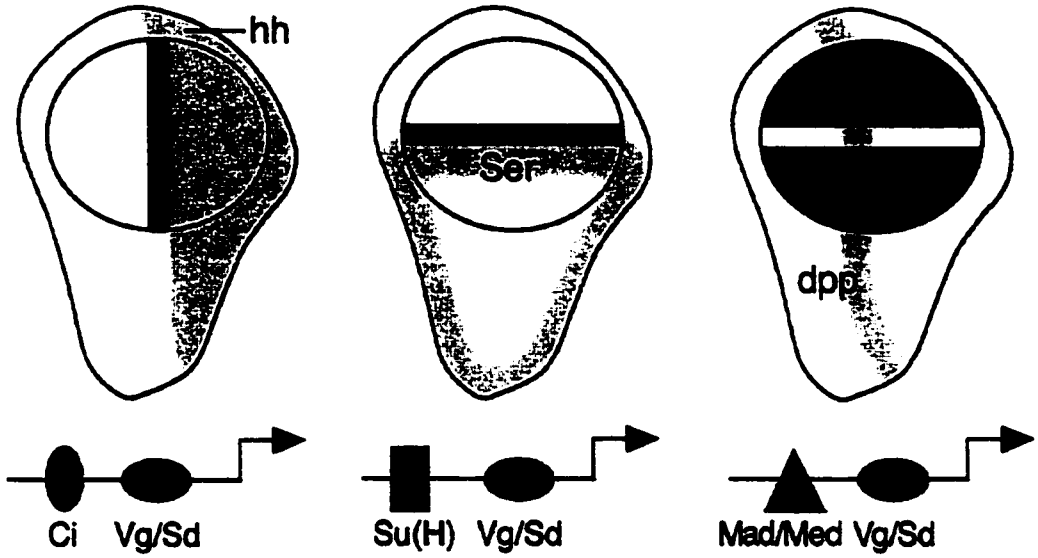
hh
Ser
dpp
Ci
Vg/Sd
Su(H)
Vg/Sd
Mad/Med
Vg/Sd

Sd/Vg complex restricts these targets to the wing field by acting with the DNA-binding transducers of specific signaling pathways on cis-regulatory elements (SRF-A, *vg*BE, *vg*QE). *hedgehog* (*hh*) is expressed in posterior cells and induces *SRF-A* in a stripe along the A/P border of the wing pouch whereby Sd/Vg restricts SRF-A within the pouch and is directly regulated by Ci. *Serrate* (*Ser*) is expressed in the dorsal portion of the wing pouch, where it promotes *Su(H)* expression that in turn activates *vg*BE. Again, the Sd/Vg protein complex limits *vg*QE activity to the pouch. Finally, *dpp* is expressed in a stripe along the A/P border and promotes *vg*QE expression in the remaining quadrants of the disc, which is contained in the pouch by Sd/Vg. This *vg*QE activity is regulated directly by Mad proteins. In each of the three examples described, the signaling proteins (Hh, Ser, and Dpp) act on specific targets (SRF-A, *vg*BE, *vg*QE, respectively). These target genes are restricted to the wing field via the Sd/Vg complex and directly regulated to give unique expression patterns by Ci, Su(H) or Mad proteins.

_vg_ expression

To revisit the idea of how the same signaling molecule induces expression of different target genes, focus will now be directed towards recent findings of how *vg* expression in the wing pouch is controlled. Here, *vg* is being affected by numerous signals involving different pathways and different genes to ultimately give normal *vg* expression in the wing pouch and therefore normal wing tissue.

As has been discussed, *vg* is required for proper formation of wing blade tissue. It has recently been shown that *homothorax* (*hth*) acts to limit where along the D/V compartment boundary wing blade development can be initiated (Casares and Mann,

2000). This limitation hence plays a defining role in the size and position of the wing blade. *hth* is suggested to accomplish this through repression of *vg*. Together, with *teashirt* (*tsh*), it has been shown that *hth* can block wing blade development by repressing some of the activities in the *Notch* pathway at the D/V boundary (Casares and Mann, 2000). Recalling that this pathway mediates the *vg*BE activity, *hth* acts indirectly through this signaling cascade to control the range of wing blade tissue.

There is a parallel activation of *vg* that is carried out by *wg* and *Notch*. These two signals activate *vg* through long and short range signaling. *wg* acts through long range signaling from the D/V border. Cells that secrete *wg* at this border induce *vg* expression. Positional information along the P/D axis within the wing blade is gained as a result of long range *wg* signaling (Zecca et al., 1996; Neumann and Cohen, 1997). Subsequently, a *vg* gradient is set up, with the highest concentration at the D/V boundary. The *Notch* short range signaling provides the manner by which *vg* is activated close to the D/V boundary within and outside the wing blade via activation of the *vg*BE (Williams et al., 1994; Kim et al., 1996).

Another recent development has been the identification of *drifter* (*dfr*) as an activator of the *vg*QE (Certel et al., 2000). The MAD-dependent activation of *vg*QE is seen in a broad expression pattern throughout the wing pouch, but is excluded from cells near the D/V boundary. The absence of expression here is due to the lack of *vg*QE activation in these cells. *dfr* is a POU domain transcriptional regulator, and with the use of the UAS-Gal4 system (UAS*dfr*, *vg*Q-lacZreporter), it was demonstrated that *dfr* is expressed in all cells within the wing pouch expressing *vg*Q-lac Z but excluded from the cells at the D/V boundary (Certel et al., 2000).

Upon broad examination of the collection of *vg* activators and repressors in the wing disc, Vg expression is dependent on at least five different signals: (1) *vg*BE binds the *Su(H)* protein in response to *Notch* signaling to restrict *vg* expression to the D/V boundary (Williams et al., 1994). (2) *vg*QE depends on a Dpp morphogen gradient, originating at the A/P boundary (Kim et al., 1996) and a signal from the D/V boundary, likely the Wg protein (Kim et al., 1996; Zecca et al., 1996), (3) autoregulatory function for Vg/Sd protein complex acting on *vg*QE (Halder et al., 1998; Klein and Arias, 1998; Paumard-Rigal et al., 1998; Simmonds et al., 1998). (4) Brinker (Brk) protein has a proposed function as a general repressor of Dpp target genes (Campbell and Tomlinson 1999; Jazwinska et al., 1999a, b), and (5)Dfr binding to a sequence element adjacent to the Mad2 binding site is essential for *vg*QE activation within the wing pouch (Certel et al., 2000).

The regulation of *vg* expression in the developing *Drosophila* wing is a complicated collage of overlapping, cooperative and distinct signals. All seem to be necessary to achieve the ultimate goal of having Vg expressed at the right time and in the right places to yield a normal adult wing.

Objectives

Work presented herein will focus on the dissection of the *vg* gene, concentrating on domains that define its activation function. The recent identification of the vertebrate homologue of *vestigial, tondu (tdu)* (Vaudin et al., 1999) has contributed some information about the functional domains of this protein. As well, within the 453 amino acids ORF (open reading frame) of *vg*, using one-hybrid assays in yeast, two activation

domains have been identified (amino acids 7-127 and amino acids 357-453. see **Figure 8**). A misexpression assay, which involves the attempt to ectopically induce *sd* expression, as well as a rescue experiment to recover flies without the mutant phenotype of *vg* will contribute to clarifying the picture of how *vg* and *sd* interact and what portions of *vg* are necessary for proper function. This will be accomplished by using portions of the *vg* ORF to see which regions are functionally important to accomplish these two tasks.

Figure 8. The *vg* ORF showing activation domains identified by Vaudin et al. 2000 are illustrated here by #1 and #2. These correspond to amino acids 7-127 and amino acids 357-453 in the Vg protein. Also shown here is the known Sd binding domain in Vg, which includes amino acids 279-335.

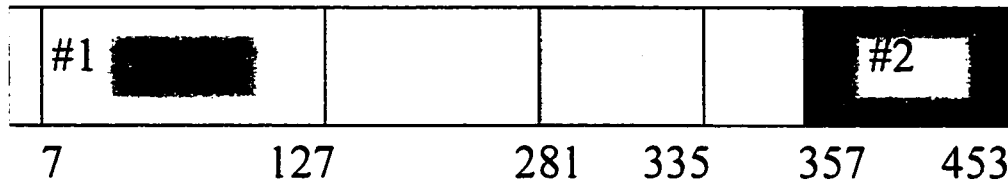
#1
#2
7
127
281
335
357
453

Materials and Methods

Drosophila stocks: origin and maintenance

All stocks and crosses were raised at 25°C. **Table 1** lists the origin of the various stocks, including their respective mutant allelic constitutions.

Construction of Δ*vg* deletions

Herein deletions will be labeled according to the primer combinations that were used in their construction along with a 'Δ' symbol to designate some extent of deletion. A schematic of the deletions made within the *vg* ORF and the corresponding deleted amino acids is shown in **Figure 9**. The shaded bars indicate regions present and open or white bars show the region deleted. A list of primer sequences and respective T_m values is shown in **Table 2**. The location of each primer within the *vg* ORF is shown in **Figure 10**. The pUAST construct was the chosen vector to carry all deletion constructs, as it contains the necessary UAS (Brand and Perrimon, 1993) to be used in assays once transformed lines were obtained. Ultimately, all constructs were used in microinjections (described below) to carry out misexpression and rescue assays.

Cloning Δ*vg* deletions from pET16b into pUAST

All deletions (excluding Δ5-5, Δ5-6, Δ5-7 and Δ5-9) were available in the pET16b (**Figure 11 A**) bacterial expression vector. These deletions had previously been constructed by Andrew Simmonds (Simmonds, 1997). Each *vg* deletion was excised from pET16b (or pUC19) using *Bam*HI restriction digestion and cloned into *Bgl*II-digested

Table 1. Summary of alleles used in experiments and their respective origins.	
Allele	**Source**
vg^{1}	Williams et al., 1991
vg^{83b27}	Williams et al., 1991
vgGal4	Hoffman and Monimura (unpublished)
sdlacZ	Bloomington Stock Centre
2506 (TM6 ^ SM1)	Bloomington Stock Centre
ptcGal4	Bloomington Stock Centre
yw	Bloomington Stock Centre

Figure 9. Deletions made within the *vg* ORF. All deletions are shown with respect to the full length construct (453 amino acids). Shaded bars represent intact regions and open bars designate areas that have been deleted. The corresponding deleted amino acids are shown on the right and the name is shown on the left hand side. Deletion names refer to primer sets used in preparation of each construct. These primers are as indicated in **Figure 12.** The known Sd binding domain (amino acids 281-335) is also shown (grey bar).

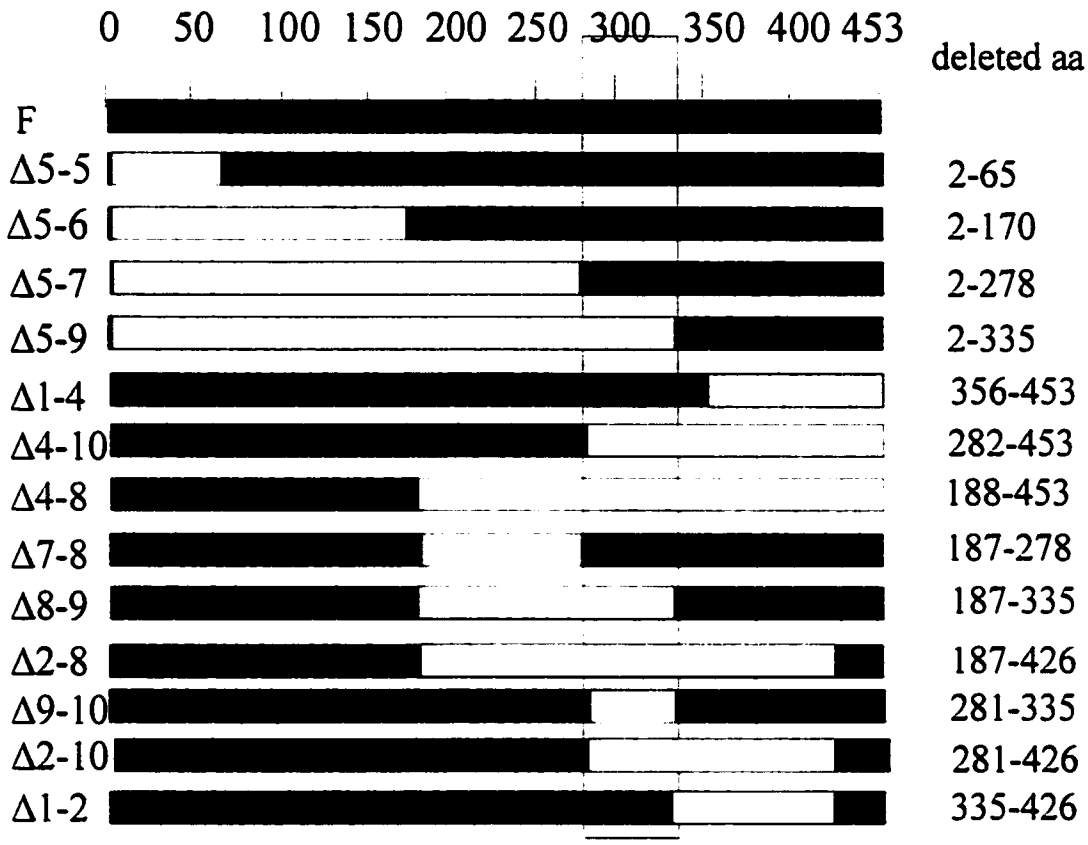
0 50 100 150 200 250 300 350 400 453
deleted aa
F
Δ5-5 2-65
Δ5-6 2-170
Δ5-7 2-278
Δ5-9 2-335
Δ1-4 356-453
Δ4-10 282-453
Δ4-8 188-453
Δ7-8 187-278
Δ8-9 187-335
Δ2-8 187-426
Δ9-10 281-335
Δ2-10 281-426
Δ1-2 335-426

Table 2. Primers utilized in making Δ*vg* constructs and corresponding T_m values.		
Primer	**Sequence 5' → 3'**	**T_m (°C)**
1	GCC**ACTAGT**CCATACAAGTCGCTA	68
2	CG**ACTAGT**GGAGTACTCCAGCTAT	68
4	CC**ACTAGT**GGAATCGTCGAAGGAT	74
5	CC**ACTAGT**ATCGGTGAGCGCAAAT	74
6	GC**ACTAGT**ACACACGCATACGCAT	74
7	GG**ACTAGT**GGGACAGGCTCAATAT	74
8	CGC**ACTAGT**ATGAGGTCCTCTTCT	74
9	GG**ACTAGT**TTACGTGCACCCCATA	74
10	CCC**ACTAGT**GAGGCCGATAGATAT	74
JMA5	CC**ACTAGT**CATCCCGGGTACCG	72

The primers were custom made by Pat Murray in the Biological Sciences Department at the University of Alberta. Sequence in bold represents the *Spe*I restriction site in each primer.

Figure 10. Primers used to make deletions within the *vg* ORF are illustrated with respect to their location and direction. The arrows indicate direction and numbers represent the primer number designation. The ATG and TAA represent the boundaries of the *vg* ORF and black arrowheads below the sequence represent intron positions within the cDNA (Williams et al., 1991).

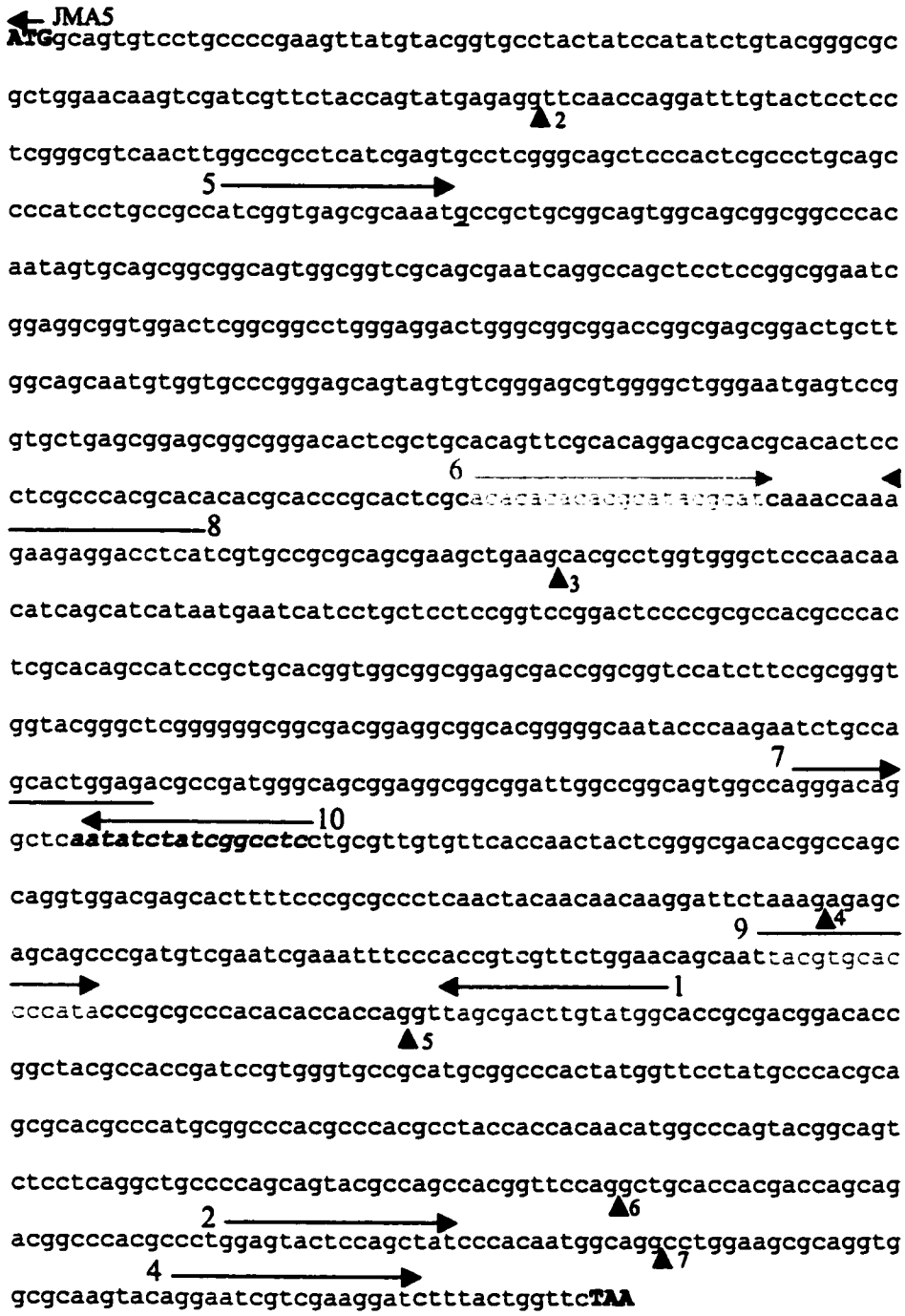
JMA5
ATGgcagtgtcctgccccgaagttatgtacggtgcctactatccatatctgtacgggcgc
gctggaacaagtcgatcgttctaccagtatgagaggttcaaccaggatttgtactcctcc
tcgggcgtcaacttggccgcctcatcgagtgcctcgggcagctcccactcgccctgcagc
cccatcctgccgccatcggtgagcgcaaatgccgctgcggcagtggcagcggcggcccac
aatagtgcagcggcggcagtggcggtcgcagcgaatcaggccagctcctccggcggaatc
ggaggcggtggactcggcggcctgggaggactgggcggcggaccggcgagcggactgctt
ggcagcaatgtggtgcccgggagcagtagtgtcgggagcgtggggctgggaatgagtccg
gtgctgagcggagcggcgggacactcgctgcacagttcgcacaggacgcacgcacactcc
ctcgcccacgcacacacgcacccgcactcgcacaaaccaaa
gaagaggacctcatcgtgccgcgcagcgaagctgaagcacgcctggtgggctcccaacaa
catcagcatcataatgaatcatcctgctcctccggtccggactccccgcgccacgcccac
tcgcacagccatccgctgcacggtggcggcggagcgaccggcggtccatcttccgcgggt
ggtacgggctcgggggggcggcgacggaggcggcacgggggcaatacccaagaatctgcca
gcactggagacgccgatgggcagcggaggcggcggattggccggcagtggccagggacag
gctcaatatctatcggcctcctgcgttgtgttcaccaactactcgggcgacacggccagc
caggtggacgagcacttttcccgcgccctcaactacaacaacaaggattctaaagagagc
agcagcccgatgtcgaatcgaaatttcccaccgtcgttctggaacagcaattacgtgcac
cccatacccgcgcccacacaccaccaggttagcgacttgtatggcaccgcgacggacacc
ggctacgccaccgatccgtgggtgccgcatgcggcccactatggttcctatgcccacgca
gcgcacgcccatgcggcccacgcccacgcctaccaccacaacatggcccagtacggcagt
ctcctcaggctgccccagcagtacgccagccacggttccaggctgcaccacgaccagcag
acggcccacgccctggagtactccagctatcccacaatggcaggcctggaagcgcaggtg
gcgcaagtacaggaatcgtcgaaggatctttactggttcTAA
1
2
3
4
5
6
7
8
9
10

Figure 11. The Δ*vg* deletions were created in pET16b (Novagen) and pUC19 (Vieira and Messing 1982). The pET16b vector **(A)** was used to clone each of the *vg* ORF deletions (except Δ5-5, Δ5-6, Δ5-7 and Δ5-9) into pUAST. A *Bam*HI restriction site was used to integrate each deletion construct into pUAST. The pUC19 vector **(B)** was used in inverse PCR reactions with full length *vg* as the template to generate deletions Δ5-5, Δ5-6, Δ5-7, and Δ5-9. The *Eco*RI and *Bam*HI restriction sites used to clone each deletion construct into pUAST are shown here. Abbreviations are as follows: Ap: ampicillin resistance, MCS; multiple cloning site, ori; origin or replication.

A

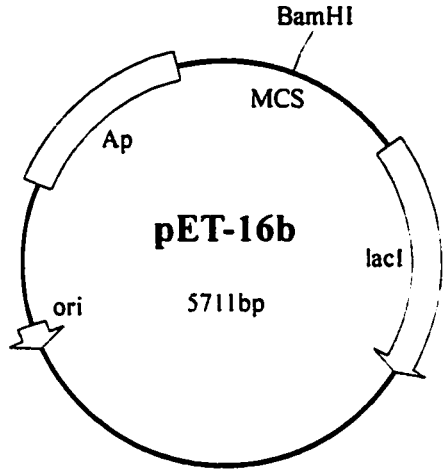
BamHI
MCS
Ap
pET-16b
lacI
ori
5711bp

B

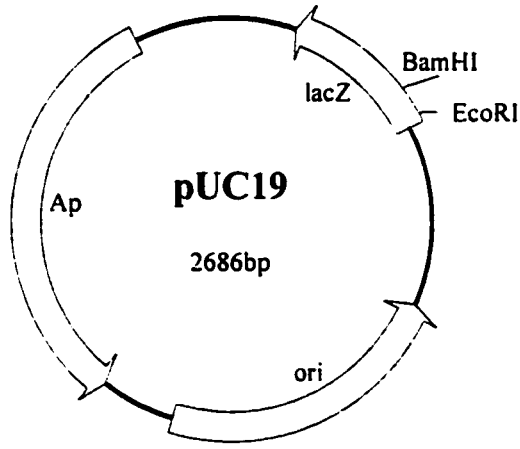
BamHI
lacZ
EcoRI
Ap
pUC19
2686bp
ori

pUAST (**Figure 12**), which was also treated with with shrimp alkaline phosphatase to prevent re-circularization. **Figure 13** summarizes this cloning assay.

Construction of Δ*vg* deletions in pUC19

To make deletions Δ5-5, Δ5-6, Δ5-7 and Δ5-9 the full-length *vg* ORF in the puc19 vector (**Figure 11 B**) was used as template. The following Taq:Pfu (20:1) PCR protocol with appropriate primer combinations. was used: 94°C for five minutes, 94°C for 30 seconds, 68 °C for one minute, 68 °C for six minutes (35 cycles), 72 °C for three minutes and held at 4 °C. The total reaction mix was 30 µl. **Figure 14** shows a flow chart of how each deletion was constructed in the pUC19 vector.

JMA-5 was constructed to include a 5' ATG in frame to the remaining ORF. This was accomplished by engineering an inner *Spe*I restriction site and an outer *Eco*RI restriction site to allow for inverse PCR (*Eco*RI ◄——— ATG *Spe*I, where arrowhead indicates direction of primer). In this manner, JMA5 was used in combinations with other primers (hypothetical primer 2, shown below) to achieve the desired deletion (indicated by the grey box below), to allow for cloning into the pUAST vector.

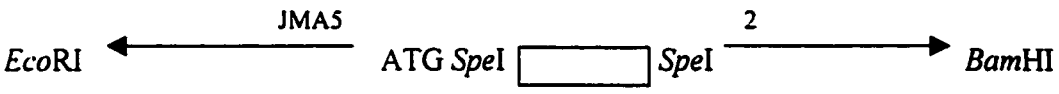

A 15 µl aliquot of PCR product was digested with *Spe*I (two hours) and loaded onto a 0.8 % agarose gel to verify the product. The linearized band was then excised from the gel and gel purified (protocol described in later section). The product was then incubated with T4 DNA ligase to assemble the deleted ORF. Mini-prep plasmid

Figure 12. All deletion constructs were cloned into pUAST (Brand and Perrimon 1993) in preparation for microinjections. The *Bgl*II and *Eco*RI sites, used as cloning sites for each Δ*vg*, the UAS driver sequence and mini white gene are shown in this representation of pUAST. The black box indicates the UAS fragment, the hatched box shows the hsp70 TATA region and the red box indicates the SV40 terminator sequence.

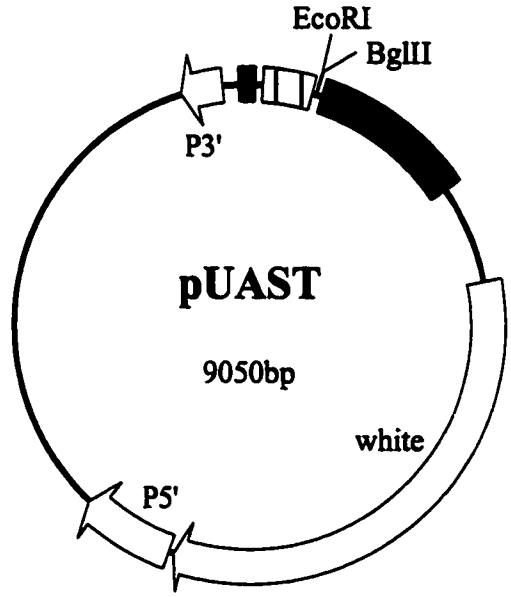
EcoRI
BglII
P3'
pUAST
9050bp
white
P5'

Figure 13. Flow chart for constructing Δ*vg* pUAST constructs. The desired deletions of *vg* were constructed in pET16b or pUC19 and then excised using *Bam*HI restriction sites (or *Bam*HI/*Eco*RI restriction sites in pUC19) and cloned into *Bgl*II (or *Bgl*II/*Eco*RI from pUC19) restriction sites in pUAST. The *Bgl*II site serves as an appropriate site for *Bam*HI integration into pUAST because it is an isoschizomer of *Bam*HI. Note that at each stage of the flow chart phrases contained in brackets represent the procedure when cloning each Δ*vg* from pUC19 to pUAST.

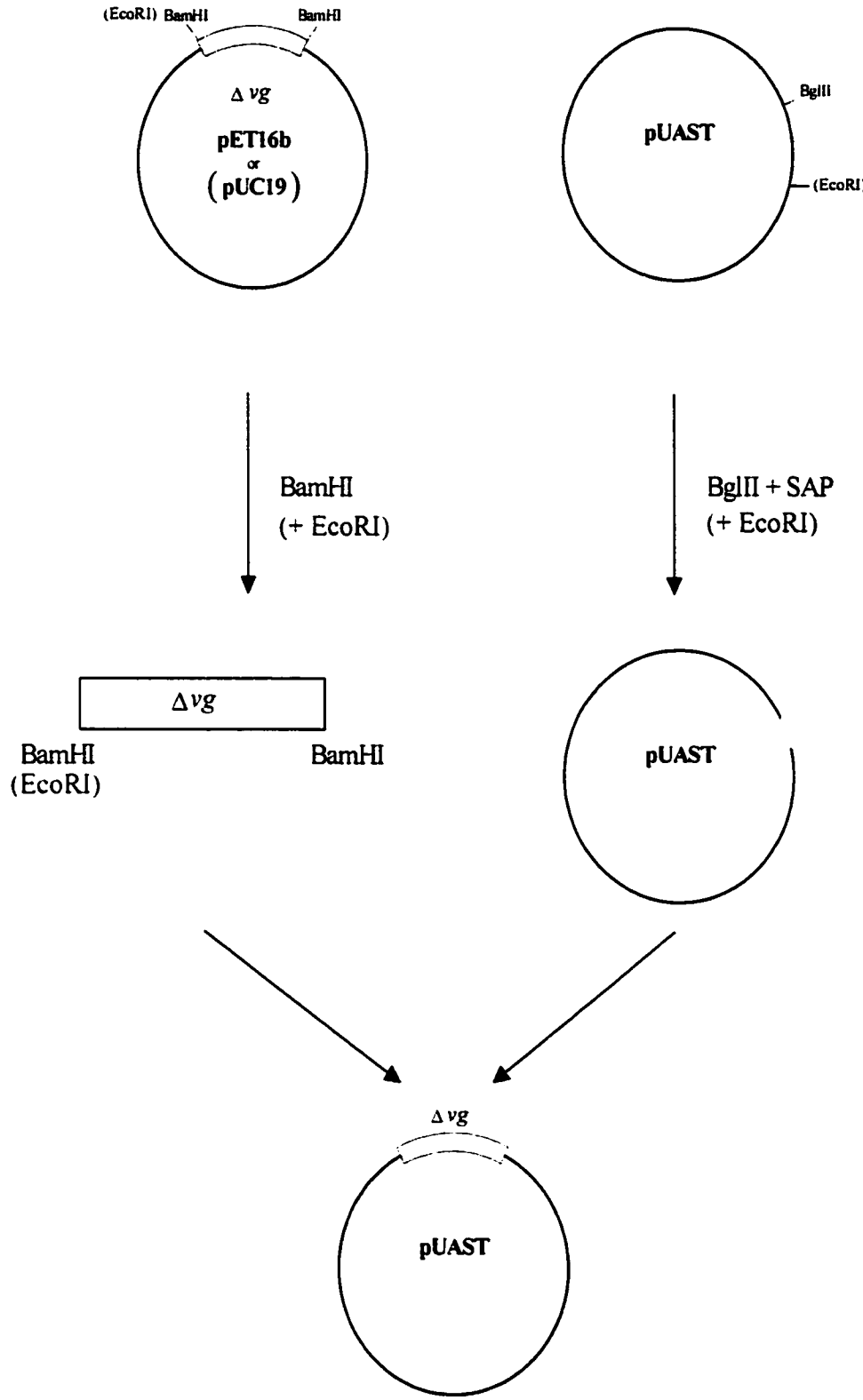
(EcoRI) BamHI
BamHI
Δ vg
pET16b
or
(pUC19)
pUAST
BglII
(EcoRI)
BamHI
(+ EcoRI)
BglII + SAP
(+ EcoRI)
Δvg
BamHI
(EcoRI)
BamHI
pUAST
Δ vg
pUAST

Figure 14. Flow chart of how each deletion was constructed in the pUC19 vector used in inverse PCR reactions. Primers 1 and 2 represent situations that were used in inverse PCR reactions to create desired deletions. Primers 1 and 2 would be chosen appropriately from those listed in **Table 2**. The shaded sequence represents the region that would be deleted in this particular reaction. All primers carried *Spe*I sites, and therefore the PCR products could be digested with *Spe*I restriction enzyme and ligated, to achieve the final deleted *vg* product in pUC19. The ORF was always maintained.

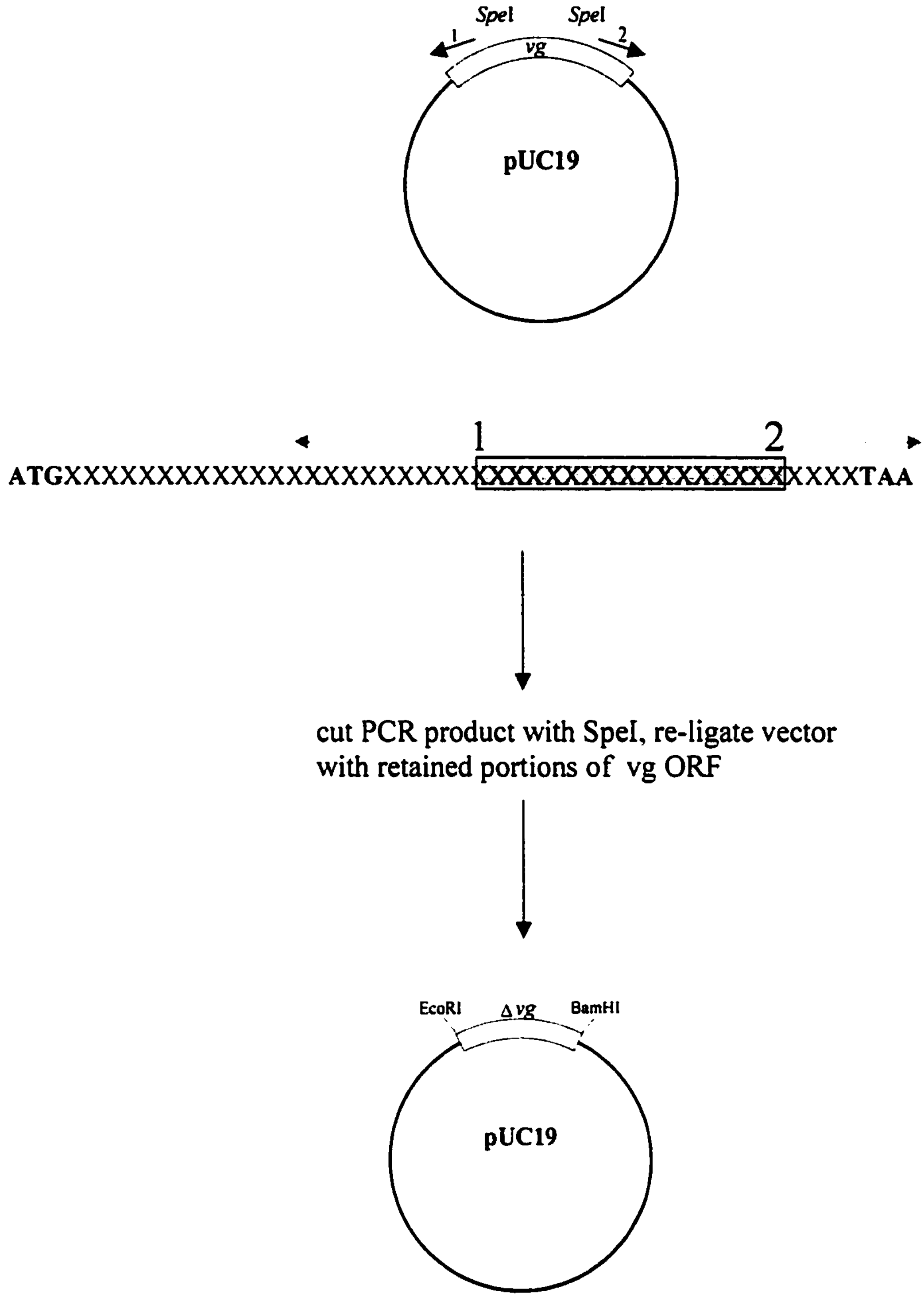
SpeI
SpeI
1
2
vg
pUC19
1
2
ATGXXXXXXXXXXXXXXXXXXXXXXXXXXXXXXXXXXXXXXXXXXXXXXXXXXXXXXXTAA
cut PCR product with SpeI, re-ligate vector with retained portions of vg ORF
EcoRI
Δ vg
BamHI
pUC19

preparations were performed on the ligated *Spe*I fragments and digested with *Bam*HI and *Eco*RI restriction enzymes to verify that the insert was present. The appropriately sized insert was excised from the agarose gel and gel purified in preparation for cloning into the pUAST vector. Sequence of each deletion construct in pUC19 was obtained to verify the product was in frame and the appropriate region had been deleted.

Figure 14 shows a flow chart of how the deletion constructs were prepared for use. Individual steps are detailed below. Each *vg* deletion was excised from pET16b using *Bam*HI and *Eco*RI restriction digestion and cloned into *Bgl*II and *Eco*RI-digested pUAST. The pUC19 vector was used in PCR reactions because it is a smaller vector and allowed for increased success when making the deletions.

Restriction digests, treatment with SAP (shrimp alkaline phosphatase), agarose gels

All restriction digests were carried out in a 37°C water bath for two hours to allow for complete cutting. Unless otherwise noted, 0.8% agarose gels were used to electrophorese samples. When treating pUAST with SAP, the vector was first digested for one hour with *Bgl*II at 37°C. After one hour the SAP was added and the sample was allowed to digest for one hour. After a total of two hours at 37°C the sample was heated to 75°C to terminate the SAP reaction and the sample was electrophoresed on an agarose gel. The resulting UASΔ*vg* constructs all had precisely defined deletions as well as two extra amino acids (serine and threonine) due to the inclusion of an in frame *Spe*I sequence in the final constructs.

DNA purification

The appropriate sized inserts were cut from the gel and dissolved in 500µl 6M NaI at 55°C. Five µl glass milk was added and then kept on ice for >45 minutes. After >45 minutes the mixture was centrifuged at 12000 rpm for nine seconds. The supernatant was decanted and the pellet resuspended in 500 µl NEET wash (100mM NaCl, one mM EDTA, five % ethanol, ten mM Tris pH 9.5) for 30 seconds and centrifuged for nine seconds (3x). After the third wash 20 µl of dH_20 was used to resuspend the pellet and this was incubated at 55°C for five minutes. After incubation, the sample was centrifuged for nine seconds and the supernatant saved. The remaining pellet was resuspended in 20 µl dH_20 and incubated at 55°C for five minutes. This sample was then centrifuged for nine seconds and added to the supernatant from the first spin. Five µl of gel purified DNA was electrophoresed on 0.8 % agarose gel before use to verify presence of product.

Ligations and transformations

A total of ten µl was used for all ligation reactions, varying the insert:vector ratio (1:3, 1:1, 3:1) in order to optimize conditions. Incubation periods were at 4 °C overnight. One in ten dilutions of the original ligation reactions were made before use in transformation protocols. Ten µl of the diluted sample was added to 100 µl of competent *E. coli* (DH5α) cells. This mixture was incubated on ice for 45 minutes, while LB-Ampicillin plates were incubated at 37°C. Samples were heat shocked at 42°C in a temp-block for 30 seconds and iced for one minute. To this, 890 µl of warmed (37°C) LB broth

was added and incubated in 37°C water bath for 30 minutes. Then, 100 µl of sample was streaked on LB-Ampicllin plates and incubated at 37°C for 8-12 hours.

Competent cell production

Competent DH5α cells were produced according to Nojima and Okayama (1990). A five ml overnight culture of LB medium was inoculated with frozen DH5 cells and grown. This culture was then inoculated with 250 ml SOB the following day and grown at 18°C with vigorous shaking until A_{600}= 0.6. Once this turbidity was, reached the flask was removed and iced for ten minutes. Then, 500 ml of this culture was transferred to a centrifuge bottle and spun for ten minutes at 4 °C (2500 x g). The pellet was then resuspended in 80 ml of ice cold TB, incubated on ice for ten minutes and then centrifuged as before. This pellet was then gently resuspended in 20 ml TB and DMSO (dimethyl sulfoxide) added with gentle swirling to a final concentration of 7%. This sample was incubated on ice for ten minutes and then dispensed into 500 µl samples and immediately chilled by immersion in liquid nitrogen. The frozen competent cells were then stored at -70°C, and thawed on ice when needed.

Mini plasmid preparations

A five ml culture of LB broth, five µl of 50mg/ml Ampicillin, and single colonies of transformed ligations was grown for 8-12 hours. A 1.5 ml aliquot of grown culture was placed in microcentrifuge tube and centrifuged at 12000 rpm for one minute. The medium was removed by aspiration and the undisturbed pellet was resuspended in 100 µl of ice cold mini-prep lysis buffer, vortexed and allowed to incubate for five minutes at

RT. To this, 200 µl of freshly prepared 0.2N NaOH, 1% SDS (for one ml: 0.2 ml 1M NaOH, 0.1 ml 10 % SDS, 0.7 ml dH_20) was added. After mixing by inversion, this was incubated on ice for five minutes. Next, 150 µl ice cold potassium acetate pH 4.8 was added, inverted to mix, incubated for 20 minutes on ice and centrifuged for five minutes at 12000 rpm and the supernatant transferred to a fresh tube. To this supernatant, RNaseA was added to a final concentration of 20 µg/ml and incubated at 37°C for 20 minutes. Then, one volume of TE-saturated phenol/chloroform was added, vortexed, and centrifuged at 12000 rpm for two minutes. The aqueous phase was then transferred to a fresh tube. One volume of chloroform:isoamyl alcohol (24:1) was added, vortexed, and centrifuged at 12000 rpm for two minutes. The upper aqueous phase was transferred to a fresh tube and 2.5 volumes 95% ethanol were added. This was mixed and precipitated for ten minutes at -70°C, and centrifuged at 12000 rpm for five minutes. The supernatant was removed and the pellet washed with 500 µl prechilled 70% ethanol, followed by centrifugation for five minutes at 12000 rpm. Finally, the vacuum dried pellet was resuspended in 40 µl dH_2O.

Maxi plasmid preparations

The remaining five ml culture used in the mini-preparation protocol was transferred to 500 ml of LB broth plus 750 µl 50 mg/ml Ampicillin in preparation for plasmid maxi preparations. After 8-12 hours of growth 250 ml of culture was transferred to 250ml-centrifuge containers and centrifuged at 10000 rpm for five minutes. The supernatant was discarded and the pellet allowed to dry slightly. The pellet was then resuspended in ten ml of buffer P1. Ten ml of buffer P2 was added, mixed by inversion,

and allowed to stand at room temperature (RT) for five minutes. Ten ml of buffer P3 was then added, mixed by inversion and incubated on ice for 20 minutes. After 20 minutes, it was spun for 30 minutes at 11000 rpm. Ten ml of equilibration buffer was added to columns during this time. The supernatant was poured through cheese cloth into columns, and allowed to gravity filter. The columns were washed with ten ml of wash buffer (2x), followed by 15 ml of elution buffer, and the eluate was collected in sterile 30 ml glass centrifuge tubes. Then, 10.5 ml isopropanol was added to the eluate and spun for 30 minutes at 11500 rpm. After this, the supernatant was discarded carefully, and the pellet was washed with RT 70 % ethanol and centrifuged for five minutes at 5000 rpm. The pellet was allowed to air dry before resuspension in 500 µl dH_20. Spectrophotometer readings were recorded to assess purity and concentration of samples.

Correct orientation

For each positive mini-preparation (that contained the correct sized deletion) further restriction digestions were used to ensure the deletion was inserted in the correct orientation. The ones identified as being in the right orientation were then used in plasmid maxi preparations. Note that maxi-preparation products were also digested in a similar fashion to ensure the appropriate construct had been purified.

Precipitation of plasmid DNA for micro-injections

Ten µg of plasmid DNA were used in all micro-injections. To ten µg DNA, two µg Δ2-3 helper vector was added and the volume brought to 30 µl with distilled water. Then, 200mM NaCl, 2.5x 95% ethanol was added to these samples. This mixture was

incubated at -70°C for approximately ten minutes and centrifuged for five minutes at 12000 rpm. The supernatant was removed carefully, the pellet washed in 200 µl 70 % ethanol and centrifuged for five minutes at 12000 rpm. The supernatant was removed and the pellet vacuum dried for two minutes before resuspending in ten µl dH_20.

Micro-injections

In preparation for micro-injections, fly population cages were assembled one to two days prior to the injection day to allow sufficient egg laying. Flies were allowed to lay on agar plates streaked with a small amount of yeast (baking yeast, water and small amount of sucrose mixed to suitable spreading consistency). Five to six microscope slides were prepared to assemble the eggs for injections as follows. A small drop of 80% glycerol was placed in the center of the slide to hold in place a cover slip. To this, home-made glue (double sided scotch tape and heptane) was added in a single strip along the two exposed sides of the cover slip. The needles used for injecting embryos were pulled with the Sutter instrument Co. Model P-87 Flaming/Brown Micropipette Puller, using 50µl disposable pipettes.

Flies were allowed to lay eggs for 45 minutes prior to injections (by replacing the bottom of the population cage with a fresh supply of yeast on a new agar plate). After 45 minutes the eggs were collected and rinsed thoroughly with dH_20 in a fine mesh screen. The embryos were then dechorionated with a 50:50 bleach: water mixture for approximately one minute with continuous agitation. These embryos were then washed thoroughly with dH_20. The embryos were then lined up along the edges of a piece of square agar, the approximate size of the cover slip, with posterior ends facing outward.

About 20 embryos per side were lined up and then transferred to the pre-glued cover slip. These embryos were dessicated in Drierite (8 mesh desiccant) for eight minutes and 15 seconds. Once dessicated, the embryos were covered with light oil (Halocarbon 56 oil) for injecting. A small amount of DNA was injected into each embryo of the appropriate stage (pre-blastoderm) and then all were covered with heavy oil (Halocarbon 700 oil) before storing at 18°C. Embryos were kept at 18°C for 48 hours and then transferred as larva to food (formula 4-24 instant *Drosophila* media from Caroline Biological Supply Company).

X-gal staining

Six to ten third instar larvae were collected and dissected by dividing into two halves and inverting the anterior portion. Then heads were transferred to 666 µl 1 X PBS (10 X PBS = 18.6mM NaH_2PO_4, 84.1 mM Na_2HPO_4 , 1750.0 mM NaCl, pH 7.4) on ice. To dissected larvae ten µl 50% gluteraldehyde was added and incubated for 20 minutes at RT. The larval heads were then washed 3x with 500 µl PBT (1 X PBS, 0.1% Triton X-100), and stained with 500 µl X-gal for 30-90 minutes at 37°C. The stain was then removed and the heads were washed 3x in 500 µl PBT. Finally, the wing imaginal discs were dissected from larvae heads and mounted in 80 % glycerol.

Antibody staining

Six to ten third instar larval heads were dissected and inverted. The dissected larvae were stored in 140 µl PBS on ice. To this, 60 µl of 10% paraformaldehyde in 1 X PBS and 250 µl heptane were added and shaken vigorously for 45 seconds. The first mix

was then drawn off with a pasteur pipette. Next, 260 µl 1 X PBS, 120 µl 10% paraformaldehyde, and 20 µl DMSO was added and the samples were shaken on a platform shaker (80 rpm) for 20 minutes. To this, 250 µl BLOCK (for ten ml, ten ml PBN-B, 0.05 g skim milk powder; PBN-B contains five ml 10 X PBS, 500 µl BSA in PBS, 250 µl NP40 for 50 ml total) was added for 90 minutes, while rocking in a cold room (4 °C). Primary antibody (was added directly to BLOCK and left overnight in a cold room on the rocker apparatus. The next day, discs were washed for 5, 10, 15, 20, and 25 minutes in PBN-B while shaking at 80 rpm. Then, 100 µl of BLOCK was added and the samples rocked in a cold room for 90 minutes. The secondary antibody was added and the samples rocked in a cold room for an additional 90 minutes. The discs were then washed 2 X for ten minutes with PBN-B and 3 X for ten minutes with PBN. A histochemical stain, using the purple alkaline phosphatase reaction (Goldstein and Fyrberg 1994) was used to detect *vg* expression. The following adjustments were made to this protocol. Embryos were washed 2 X 5 minutes in alkaline phosphatase buffer. A 300 µl aliquot of BCIP/NBT solution (diluted ½) was added to the embryos. This reaction took approximately 15-20 seconds, after which it was stopped by washing 2 X one minute with alkaline phosphatase buffer. The embryos were then incubated in 70% glycerol overnight before mounting the discs in 80% glycerol.

UAS-Gal4 system

The UAS-Gal4 system, identified by Brand and Perrimon (1993), is a very powerful tool able to be used in *Drosophila*. The Gal4 DNA binding protein of yeast and the upstream activating sequences (UAS) to which it binds are the components that allow

this tool to work. This method allows one to misexpress a cloned coding region in a selected pattern, which is conferred by the chosen driver (in this case *ptc*Gal4 driver). This system enables one to select where and at what time you wish to express a particular coding region. This type of control allows for very distinct examinations of ectopically expressing a particular gene. This system was used in the two assays discussed below.

Misexpression

The cross used to examine Sd misexpression in the UAS Δ*vg* lines is shown in **Figure 15**. To assay for the presence of ectopic Sd expression (using X-gal staining as described) the *ptc*Gal4 driver was utilized in combination with *sd*lacZ and the presence of an ectopic stripe (equivalent to *ptc* expression along the A/P border of the wing disc) was looked for in wing discs.

Rescue of *vg* phenotypes

To examine which deletions were capable of rescuing either the vg^{83b27} or vg^{1} mutants, a stock of UASΔ*vg* flies in a *vg* background was generated. A translocation second and third chromosome balancer (2606) was used, as the location of UASΔ*vg* was unknown. The UAS*vg* in *vg* background flies were crossed to *vg*;*vg*GAL4 flies and the progeny generated from this cross was assessed for varying degrees of rescue ability.

Figure 15. The cross used in mixexpression assays is shown. The *2506 chromosome represents a second and third chromosome balancer (TM6 ^ SM1). This chromosome carries Tb (identified by tubby larvae) and Hu (adult flies have humeral bristles, or a hairy shoulder phenotype). Thus, in the progeny resulting from the cross shown here, all non-Tubby larvae were experimental (contain UASΔ*vg* and *sd*lacZ;*ptc*Gal4). The *ptc* expressin pattern is contained in a thin stripe along the A/P border of the wing disc and will be the site at which UASΔ*vg* will be ectopically expressed.

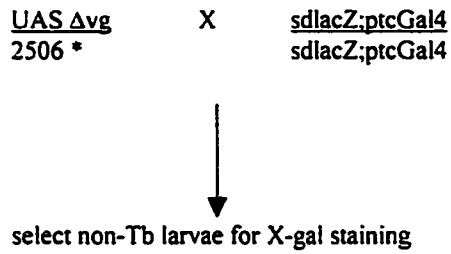
UAS Δvg
X
sdlacZ;ptcGal4
2506 *
sdlacZ;ptcGal4
select non-Tb larvae for X-gal staining

Results

Construction of Δ*vg* deletions

To perform the two important assays for examining regions of the *vg* ORF necessary for (1) Sd misexpression and (2) rescue ability of *vg* mutants, it was necessary to clone each deletion into the pUAST vector (Brand and Perrimon, 1993). These UASΔ*vg* constructs could then be micro-injected into flies and utilized in examining directed misexpression via the UAS-Gal4 system (Brand and Perrimon, 1993). This was accomplished by sub-cloning each deletion from pET16b into pUAST, via *Bam*HI restriction sites. As this was non-directional cloning, the orientation of each resulting product had to be assessed before introducing the UAS construct into flies. Problems were encountered, whereupon it was realized that all deletion constructs actually contained the deleted *vg* ORF in the wrong orientation in the pUAST vector. Upon this realization, all constructs were re-made and re-injected. Verification that constructs were assembled in the 'right' orientation was seen using the full length *vg* in misexpression and rescue experiments. As the full length *vg* construct would be able to provide the full ORF, positive Sd misexpression and wing rescue should have been observed when using this construct in the respective experiments.

This problem was not encountered with four deletion constructs (Δ5-5, Δ5-6, Δ5-6, and Δ5-9). These constructs were not available in pET16b as useful deletions. In particular, they did not include the 5'ATG start site, and therefore had to be re-constructed. This was carried out using the pUC19 vector, as described in the materials and methods. Importantly, these deletions utilized directional cloning into pUAST via

*Eco*RI and *Bam*HI restriction sites from pUC19 into *Eco*RI and *Bgl*II restriction sites of pUAST (*Bgl*II is an isoschizimer of *Bam*HI).

Δ*vg* lines

Table 3 summarizes the lines that were generated for each deletion and the chromosomal location of each. Each transformant indicated with a different number (1, 2, 3, etc.) represents an independently collected line. Homozygous UASΔ*vg* / UASΔ*vg* stocks were established for each independent line. All experiments discussed herein were performed with all available lines. Apparently, no transformant disrupted a vital genomic region, since it was possible to produce homozygotes of each transformant.

Sd misexpression

It is known that there is a physical interaction between Vg and Sd and that Vg is postulated to serve as the TIF which governs the ability of Sd to provide activation or repression activity (as does its human homologue, TEF-1) (Simmonds et al., 1998). Sd has also been shown to target Vg to the nucleus (Halder et al., 1998, Simmonds et al., 1998). Thus, to investigate what regions of the 453 amino acid ORF of *vg* are necessary to accomplish other functional aspects of Vg, a misexpression assay was devised that utilized the UAS-Gal4 system (Brand and Perrimon, 1993). The deleted UASΔ*vg* fragments would be activated in cells where Gal4 is expressed (eg. by *ptc*Gal4), and because *sd*lacZ is included as part of the genotype of experimental organisms, the resulting larvae stained with X-gal would be representative of UASΔ*vg* being able to

Table 3. Summary of transformed lines and corresponding chromosomal locations.		
Deletion	**Transformed line♦**	**Chromosomal location**
Full length	1	II
	2	II
pUAST	1	II
Δ1-2	1	II
	2	II
	3	II
Δ1-4	1	II
	2	II
	3	X
Δ2-8	1	II
	2	II
Δ2-10	1	X
	2	II
	3	II
	4	III
Δ4-8	1	III
	2	II
	3	II
	4	III
Δ4-10 *	1	II
Δ5-5	1	III
	2	III
Δ5-6	1	II
	2	X
	3	III
	4	X
Δ5-7	1	III
	2	III
	3	II
	4	II
Δ5-9	1	X
	2	II
Δ7-8	1	II
	2	II
	3	X
	4	II
	5	III
	6	X
Δ8-9	1	X
	2	II
Δ9-10	1	III
	2	III

♦The column titled 'transformed line' refers to independent lines that were collected for a particular construct. *Δ4-10 resulted in only one transformed line.

induce ectopic Sd expression (detected via β-galactosidase reaction with lacZ) in a *ptc* expression pattern.

To successfully use the assay, it was necessary to first generate larvae that were of the genotype UASΔ*vg* / *sd*lacZ;*ptc*Gal4. This was done by performing the cross described in **Figure 15**. By selecting non-Tb larvae, one could be assured that they would have the wanted UASΔ*vg* / *sd*lacZ;*ptc*Gal4 genotype. The results of using this analysis with all deletion constructs are described below.

The corresponding wing imaginal discs, stained with X-gal, are shown in **Figures 16, 17, 18** and **19**. It should be noted that only one representative line of each construct is shown in these figures. In each case the specific deleted region is shown above the wing disc, indicating which amino acids are deleted in comparison to the full length 453 amino acid ORF. The full length *vg* construct staining is shown in **Figure 16,** and gives a misexpression pattern, as expected. This ectopic *sd*lacZ pattern is co-extensive with the ectopic UAS*vg* pattern driven by *ptc*Gal4 (Simmonds et al., 1998). Compiled in **Figure 17** are the deletion constructs which gave positive misexpression in this assay, along with their respective deleted amino acids. In panel A, the result from deletion Δ5-5 (amino acids 2-65 deleted) is shown. This construct produced some misexpression, although it was not as intense as that produced from the full length *vg* ORF. When further deletions are made within the same region, as in deletions Δ5-6 (amino acids 2-170 deleted) and Δ5-7 (amino acids 2-278 deleted), an even weaker misexpression is observed (**Figure 17 B** and **C**, respectively). This weak staining activity is especially faint in deletion Δ5-7. Although all of these constructs show lesser activity

Figure 16. Sd mixexpression assay results are illustrated here. The full length *vg* construct used in the misexpression assay gave the illustrated response to staining with X-gal for 1.5 hrs (wing discs are mounted in 80% glycerol). The endogenous normal Sd expression is slightly darker and is manifest as a crescent over the D/V boundary of the wing disc. The ectopic Sd expression is represented by a vertical stripe along the A/P boundary. where *ptc* expression (that is driving *vg* expression) is located.

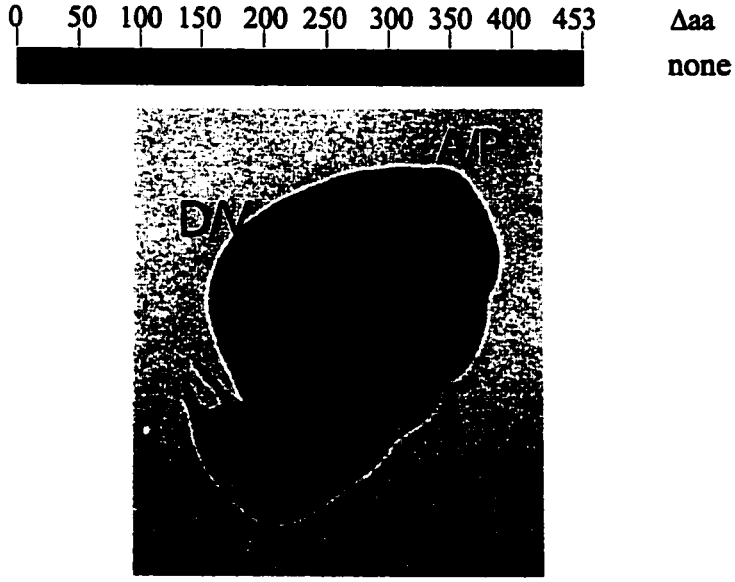
0 50 100 150 200 250 300 350 400 453
Δaa
none

Figure 17. Deletion constructs showing positive misexpression activity (indicated by black arrowheads) are summarized here. The deleted amino acids for each construct are on the right of the respective wing discs by way of deletion bar diagrams. **(A)** Δ5-5 (amino acids 2-65 deleted), **(B)** Δ5-6 (amino acids 2-170 deleted), **(C)** Δ5-7 (amino acids 2-278 deleted), **(D)** Δ7-8 (amino acids 187-278 deleted), **(E)** Δ1-4 (amino acids 356-453 deleted), and **(F)** Δ1-2 (amino acids 335-426 deleted). Each wing disc shows the corresponding deleted amino acids compared to full length *vg*.

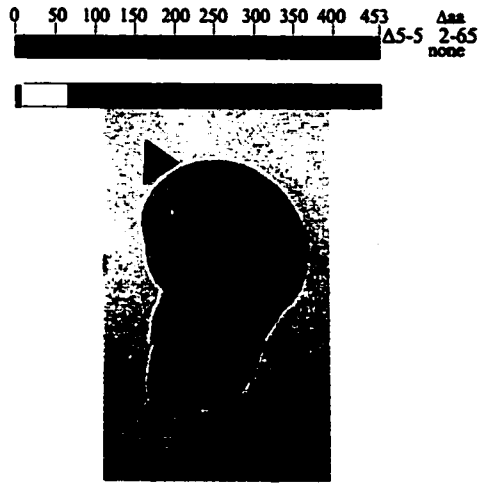
0 50 100 150 200 250 300 350 400 453
Δaa
Δ5-5 2-65
none

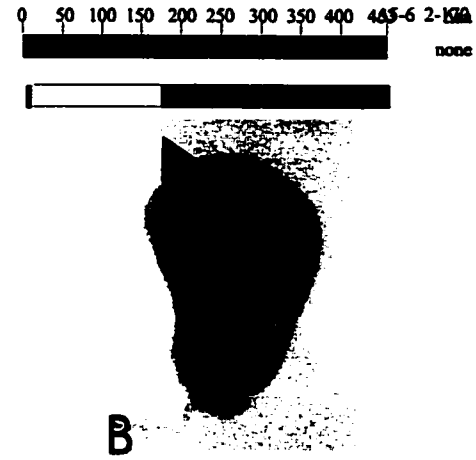
0 50 100 150 200 250 300 350 400 453
none
B

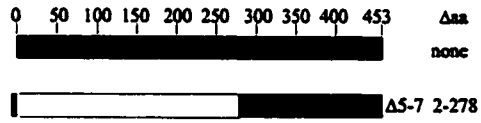
0 50 100 150 200 250 300 350 400 453
Δaa
none
Δ5-7 2-278

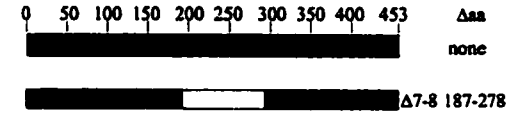
0 50 100 150 200 250 300 350 400 453
Δaa
none
Δ7-8 187-278


C


D

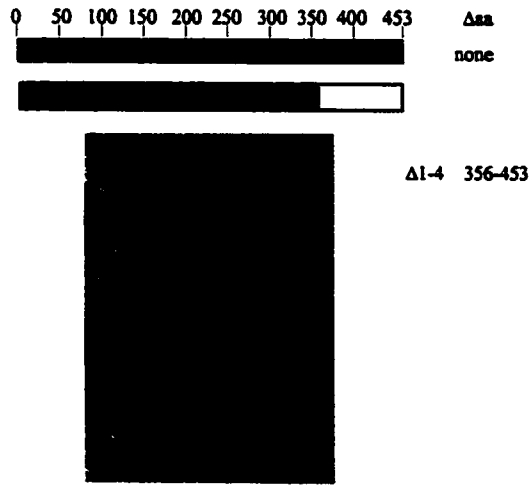
0 50 100 150 200 250 300 350 400 453
Δaa
none
Δ1-4 356-453

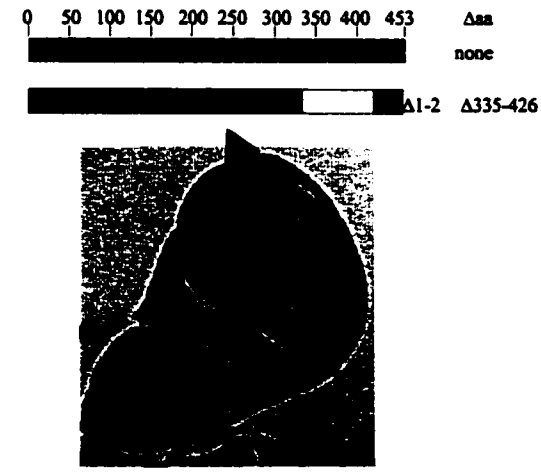
0 50 100 150 200 250 300 350 400 453
Δaa
none
Δ1-2 Δ335-426

Figure 18. Deletion constructs that gave no Sd misexpression activity are illustrated. **(A)** pUAST, control, **(B)** Δ5-9 (amino acids 2-335 deleted), **(C)** Δ4-10 (amino acids 282-453 deleted), and **(D)** Δ4-8 (amino acids 188-453 deleted). Each wing disc panel shows the corresponding deleted amino acids compared to full length *vg*. The sd binding domain of Vg lies within amino acid residues 281-335. Thus, each of the deletion constructs portrayed in the figure removed the Sd-binding domain as well as other regions of the *vg* ORF.

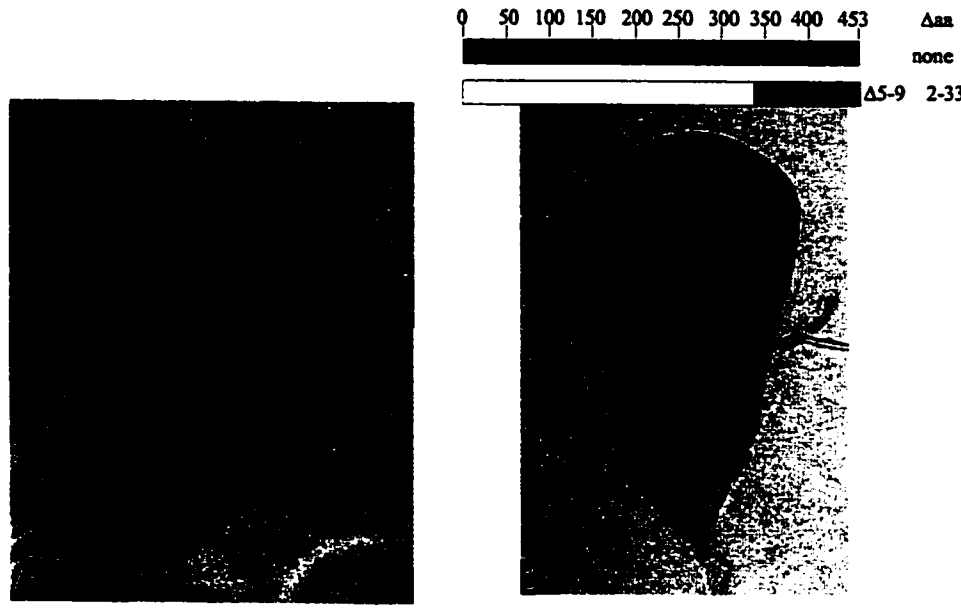
0 50 100 150 200 250 300 350 400 453 Δaa
none
Δ5-9 2-335

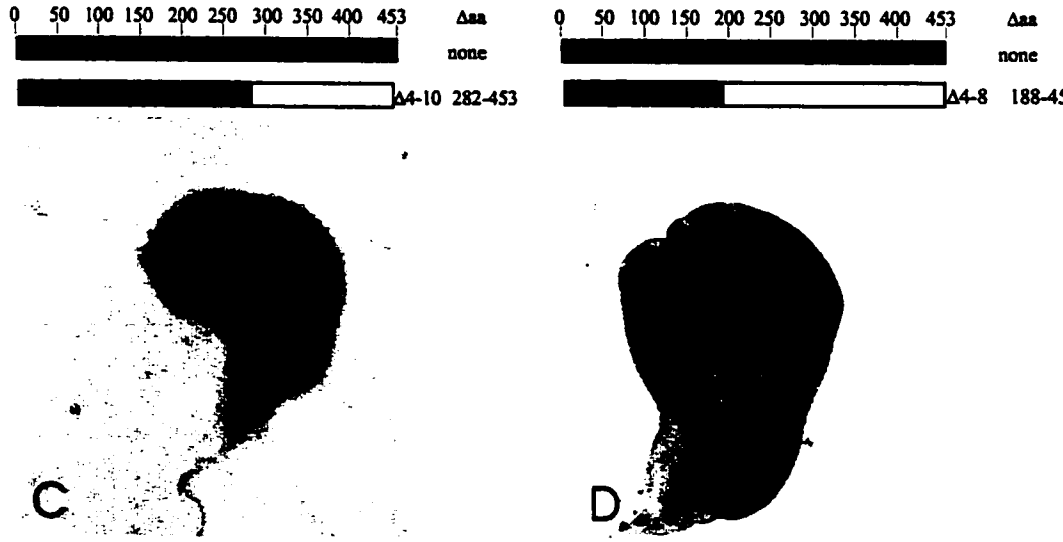
0 50 100 150 200 250 300 350 400 453 Δaa
none
Δ4-10 282-453
0 50 100 150 200 250 300 350 400 453 Δaa
none
Δ4-8 188-453
C
D

Figure 19. Remaining deleted *vg* constructs that gave no Sd misexpression activity. **(A)** Δ8-9 (amino acids 187-335 deleted), **(B)** Δ2-8 (amino acids 187-426), **(C)** Δ9-10 (amino acids 281-335 deleted), and **(D)** Δ2-10 (amino acids 281-426 deleted). Each wing disc panel shows the corresponding deleted amino acids compared to full length *vg*. Again, each of these Δ*vg* constructs deleted the Sd-binding domain plus other regions of the *vg* ORF.

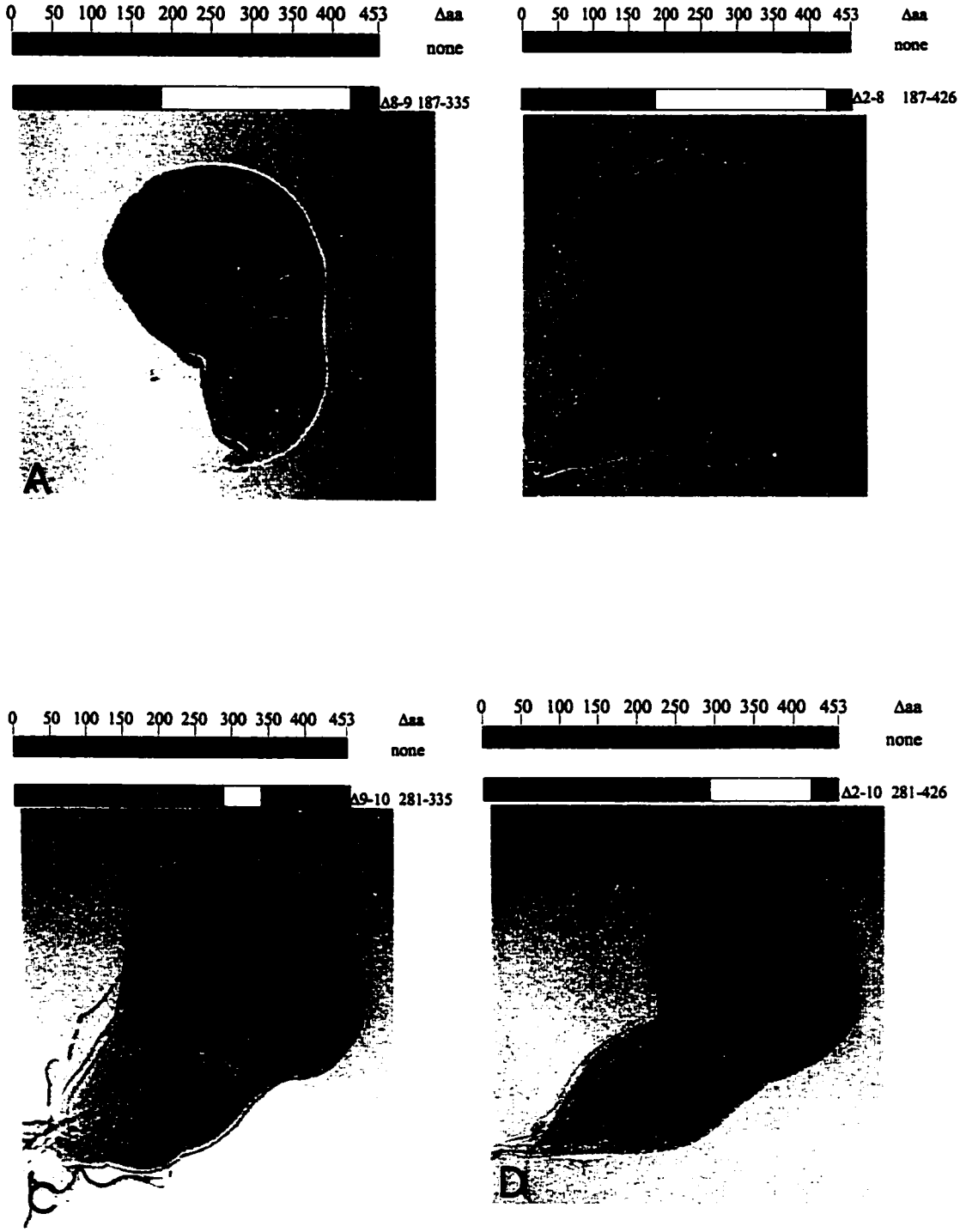
0 50 100 150 200 250 300 350 400 453
Δaa
none
Δ8-9 187-335
A
0 50 100 150 200 250 300 350 400 453
Δaa
none
Δ2-8 187-426
0 50 100 150 200 250 300 350 400 453
Δaa
none
Δ9-10 281-335
C
0 50 100 150 200 250 300 350 400 453
Δaa
none
Δ2-10 281-426
D

than full length *vg*, staining could be detected. In deletion Δ7-8 (amino acids 187-278 deleted) the misexpression activity is comparable to that of the full length *vg* (**Figure 17 D**). Examination of constructs Δ1-4 (amino acids 356-453 deleted) and Δ1-2 (amino acids 335-426 deleted) also show misexpression activity (**Figure 17 E, and F**).

Figures 18 and **19** summarize the deletion constructs that failed to give positive results in the misexpression assay. As previously noted, each wing disc is shown with its corresponding deleted amino acids compared to the full length Vg. The first wing disc shown in **Figure 18 A**, is the negative control for this assay, which is the result of using the pUAST vector as the injected construct. No misexpression activity is detected using this control. In **Figure 18 B**. deletion Δ5-9 (amino acids 2-335 deleted). the ability to activate Sd misexpression is also lost. Deletions Δ4-10 and 4-8 (deleted amino acids 282-453 and amino acids 218-453, respectively) do not show any misexpression (**Figure 18 C** and **D**, respectively) either. Finally, there is no misexpression seen in deletions Δ8-9, Δ2-8. Δ9-10. or Δ2-10 (deleting amino acids 217-335, 217-426, 281-335 and 281-426, respectively). These wing imaginal discs are shown in **Figure 19 A, B, C**. and **D**. respectively. **Table 4** summarizes the results from the misexpression assay for each deletion.

vg antibody staining

To ensure that when looking at the results of the Sd misexpression assays that *vg* was indeed being produced along the *ptc* expression pattern in the wing discs, *vg* antibody staining was performed. This was done to verify that negative results (i.e. no

Table 4. Summary of ability of deletion constructs to misexpress Sd.		
Deletion designation	**Amino acids deleted**	**Misexpression of sdlacZ by ptcGal4/UASΔvg (yes/no)**
Full length	none	yes
Δ1-2	335-426	yes
Δ1-4	356-453	yes
Δ2-8	187-426	no
Δ2-10	281-426	no
Δ4-8	188-453	no
Δ4-10	282-453	no
Δ5-5	2-65	yes (weak)
Δ5-6	2-170	yes (very weak)
Δ5-7	2-278	yes (very weak)
Δ5-9	2-335	no
Δ7-8	187-278	yes
Δ8-9	187-335	no
Δ9-10	281-335	no

Deletions are named according to primer combinations used and the ability to accomplish misexpression is noted as present or absent, with three notably weaker lines (Δ5-5, Δ5-6 and Δ5-7). Misexpression of *sd*lacZ represents ectopic induction of *sd* induced by an underlying ectopic induction of *vg* by the *ptc*Gal4 driver.

*sd*lacZ staining detected along *ptc* A/P 'stripe') were not simply due to lack of Vg production.

Those constructs that are expected to be able to be stained with *vg* antibody (domain 2) were tested using a histochemical stain, alkaline phosphatase, which produced a purple reaction product. The *vg* antibody domain 2 is specific for amino acids 180-453 of the *vg* ORF (Williams et al., 1991). The deletions that we expected to stain included the full length construct, Δ5-5, Δ5-6, Δ5-7 and Δ7-8. The results for each of these constructs are shown in **Figure 20** (**A, B, C, D**, and **E**, respectively). All other deleted constructs removed too much of the *vg* ORF to be detected. All tested constructs are the result of staining larvae that had the UAS*vg* ; *sd*lacZ ; *ptc*Gal4 genotype. From the results, we infer that *vg* expression was present in the normal *vg* and ectopic *ptc* expression patterns for all the tested constructs, despite our inability to confirm this for a number of the constructs.

_vg_ mutant rescue

Aside from examining the ability of deletion constructs to misexpress Sd, it was also of interest to investigate what portions of the *vg* ORF were necessary to provide rescue of *vg* mutant phenotypes. Two recessive mutants were selected for this study, vg^{83b27} and vg^{1}. These two mutants are stable lines and vary with respect to severity of vestigial phenotype. In vg^{83b27} flies, there is little to no wing tissue present, whereas in vg^{1} mutants, minimal wing tissue is present (see **Figure 6** for mutant phenotypes). Again, the UAS-Gal4 system (Brandt and Perrimon, 1993) was utilized in these experiments. In this scenario, each UASΔ*vg* deletion construct would be expressed in cells also

Figure 20. *vg* antibody staining (alkaline phospatase) results are shown here. Verification that *vg* is being expressed in the deleted constructs is determined by the presence of the ectopic stripe of *vg* in the ptc expression pattern in larvae stained from a sdlacZ;ptcGal4 x UASΔvg cross. Constructs able to be tested this way included full length *vg* **(A)**, Δ5-5 **(B)**, Δ5-6 **(C)**, Δ5-7 **(D)** and Δ7-8 **(E)**. Arrowheads indicate the Vg detection in a *ptc* expression pattern.

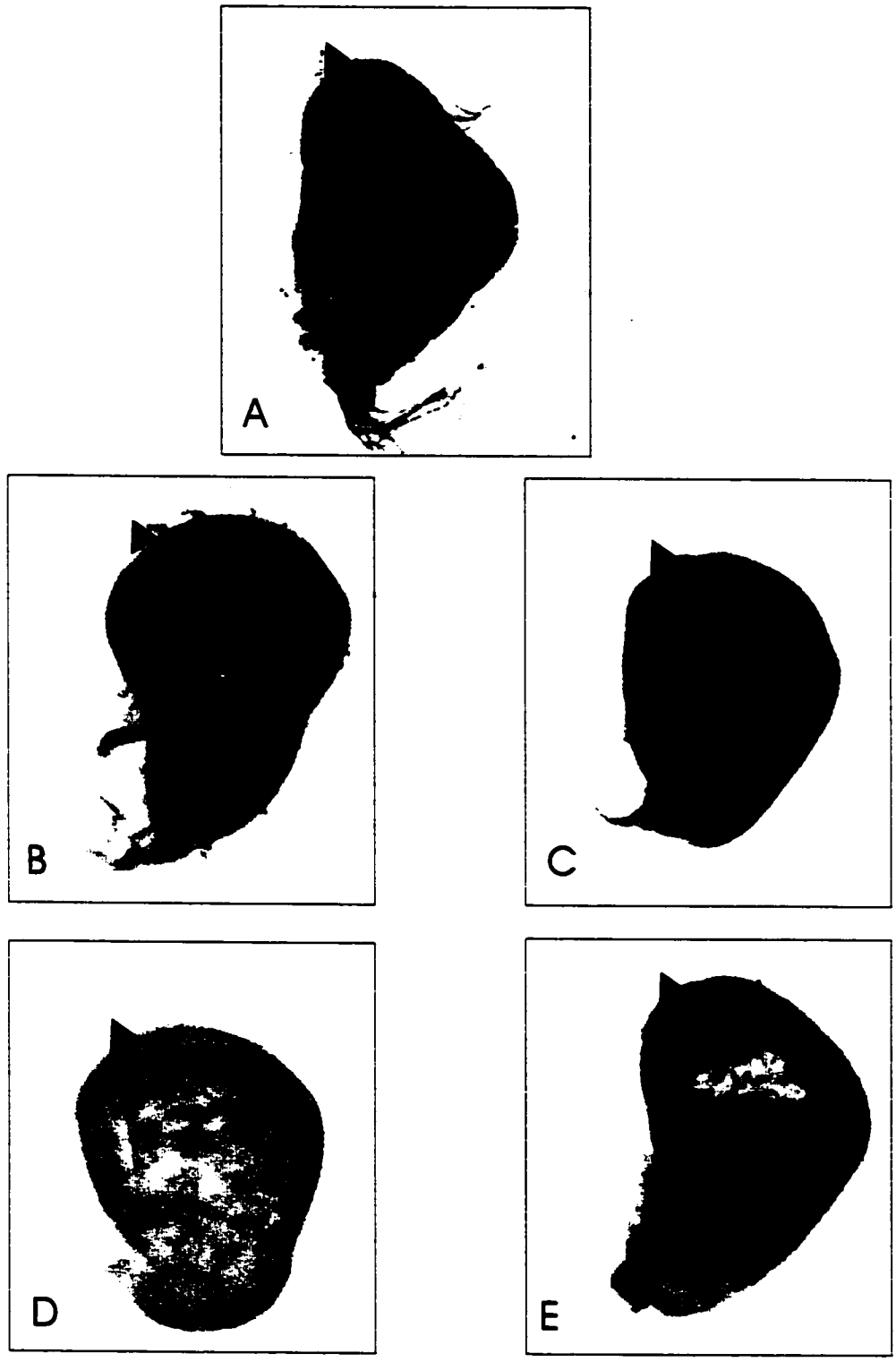
A
B
C
D
E

containing a *vg*Gal4 construct (either vg^{83b27};Gal4 or vg^{1};Gal4 was used). In this manner, the UASΔvg deletions would be driven by *vg*Gal4 in a *vg* background, and provide mutant flies with some portion of the *vg* ORF. The flies from this cross could then be examined for the extent of wing tissue rescued, compared to the appropriate respective mutant starting phenotype.

In order to use this UAS-Gal4 assay, a UASΔvg / UASΔvg genotype needed to be generated for each deletion, in a *vg* mutant background. These lines could then be used to cross to *vg*;*vg*Gal4 (vg^{83b27} or vg^{1}) to examine rescue ability. Thus, all tested flies were homozygous for either vg^{83b27} or vg^{1} and any wing restoration would be due to *vg*Gal4 driving the expression of the various UASΔvg constructs.

The corresponding rescued wing phenotypes are shown in **Figure 21** and **22** (vg^{83b27} and vg^{1}, respectively). Again, each deletion line is represented with one wing photograph. Only the deletion constructs that were able to give any degree of rescue ability are shown in **Figure 21** and **22**. All other deletion constructs showed no rescue ability and the phenotype of these are comparable to the phenotypes of vg^{83b27} or vg^{1}. There was some variability in progeny resulting from rescue by the Δvg constructs. This variability was minimal, where at least 90% of the flies from a given cross showed similar degrees of rescue.

Figure 21. Wing rescue of vg^{83b27} mutants. The deleted constructs that were able to provide rescue for this mutant are shown here. The deleted amino acids for each construct are listed in brackets. **(A)** full length *vg* (no amino acids deleted), **(B)** Δ5-5 (amino acids 2-65 deleted), **(C)** Δ5-6 (amino acids 2-170 deleted), **(D)** Δ5-7 (amino acids 2-278 deleted), **(E)** Δ1-4 (amino acids 356-453 deleted), **(F)** Δ7-8 (amino acids 187-278 deleted), and **(G)** Δ1-2 (amino acids 335-426 deleted).

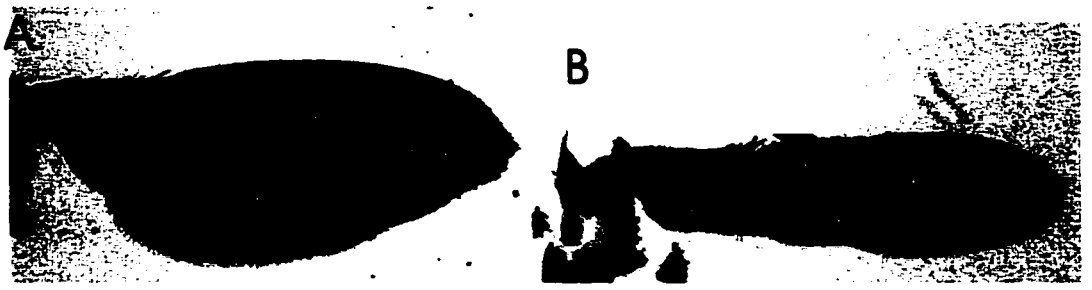
A
B

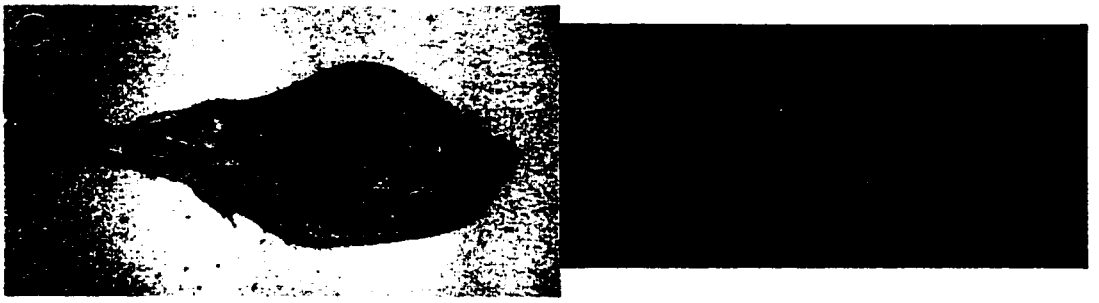


C

Figure 22. Wing rescue of vg^{1} mutants. The deleted constructs that were able to provide rescue for this mutant are shown here. The deleted amino acids for each constructs are listed in brackets. **(A)** full length *vg* (no amino acids deleted), **(B)** Δ5-5 (amino acids 2-65 deleted), **(C)** Δ5-6 (amino acids 2-170 deleted), **(D)** Δ5-7 (amino acids 2-278 deleted), **(E)** Δ1-4 (amino acids 356-453 deleted), **(F)** Δ7-8 (amino acids 187-278 deleted), and **(G)** Δ1-2 (amino acids 335-426 deleted).

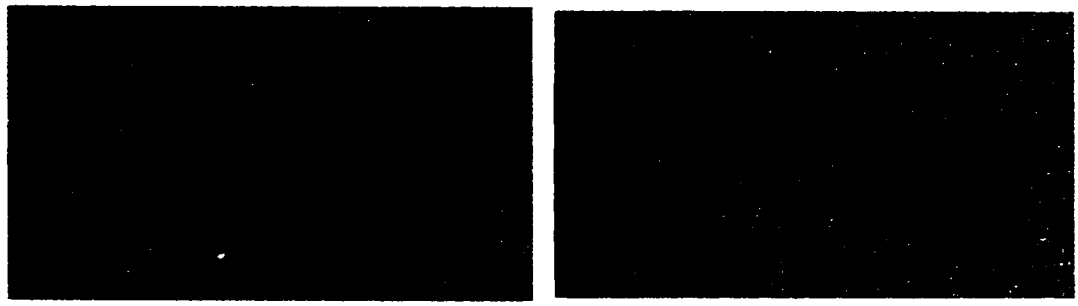

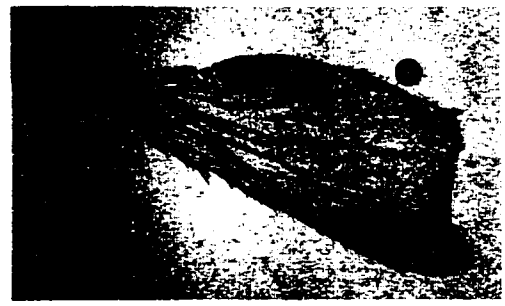

vg^{83b27} rescue

The extent to which the full length *vg* construct was able to rescue vg^{83b27} is shown in **Figure 21 A.** When the first 65 amino acids are deleted (excluding ATG), as in Δ5-5, the rescued wing is not as complete as that of the full length *vg*, but compared to vg^{83b27} is significant (**Figure 21 B**). Further deletions in this region give a somewehat lesser ability to rescue vg^{83b27}, as is seen in the constructs Δ5-6 and Δ5-7, which delete amino acids 2-170 and 2-278, respectively (**Figure 21 C** and **D**, respectively). The amount of wing tissue in the rescued Δ5-6 wings (**Figure 21 C**) is decreased, compared to Δ5-5, and wings show blistering. The Δ5-7 deletion rescued wings show less wing tissue than any other rescued lines, but more than the vg^{83b27} mutant. The wings in Δ1-4 rescued flies (deleting amino acids 356-453, **Figure 21 E**) somewhat better than those of deletion Δ5-5 (**Figure 21 B**). The ability of Δ7-8 to rescue vg^{83b27} is improved even more and is comparable to that of the full length *vg* (deletes amino acids 187-278, **Figure 21 F**). Finally, deletion Δ1-2, which deletes amino acids 335-426, shows a moderate rescue of vg^{83b27} (**Figure 21 G**), comparable to **Figure 21 E.**

vg^{1} rescue

Results pertaining to vg^{1} rescues are illustrated in **Figure 22.** A representative rescued wing for each construct is shown. The full length *vg* construct was able to produce a substantial wing rescue of the vg^{1} phenotype (**Figure 22 A**). All deletions listed herein maintained the Sd binding domain (amino acids 279-335). When amino acids 1-65 (excluding ATG) are deleted, as in Δ5-5, wing rescue is not as extensive as full

length. but more wing tissue than that in the vg^{1} mutant is present (**Figure 22 B**). Further deletions within this region (Δ5-6 and Δ5-7. deleting amino acids 2-170 and 2-278. respectively) again show weak rescue, but also exhibit more wing tissue than the mutant phenotype (**Figure 22 C, D**, respectively). The deletion Δ1-4 deletes amino acids 356-453. and corresponds to the wing rescue shown in **Figure 22 E**. The Δ7-8 deletion gives a very good wing rescue. as shown in **Figure 22 F** and deletes only amino acids 187-278. The final construct that was able to give rescue to vg^{1} mutants is shown in **Figure 22 G**. The Δ1-2 construct (deletes amino acids 335-426) is able to give some wing rescue.

Table 5 summarizes the ability of the various lines of Δ*vg* to rescue vg^{83b27} and vg^{1}. All of the deletions not mentioned in the vg^{83b27} and vg^{1} results failed to provide wing rescue of the two mutants. The deletions that did not rescue vg^{83b27} were also the same deletions that did not rescue vg^{1}. In each case where no rescue was seen. the Sd binding domain had been deleted. The negative control. as used in the misexpression assay (injected pUAST vector alone). was included in rescue experiments and gave no wing rescue for either vg^{83b27} or vg^{1}.

Figure 23 summarizes the domains of the *vg* ORF that were required for both Sd misexpression and rescue. These regions were consistent between these two assays (amino acids 1-170, 279-335 and 336-453).

Table 5. Summary of the ability of deletions to rescue the vg^{83b27} or vg^{1} phenotype.		
Deletion	**Rescue ablity (yes/no)** vg^{83b27}	vg^{1}
Full length	yes	yes
Δ1-2	yes	yes
Δ1-4	yes	yes
Δ2-8	no	no
Δ2-10	no	no
Δ4-8	no	no
Δ4-10	no	no
Δ5-5	yes	yes
Δ5-6	yes	yes
Δ5-7	yes	yes
Δ5-9	no	no
Δ7-8	yes	yes
Δ8-9	no	no
Δ9-10	no	no

The various deletions are listed according to primer names and rescue ability is either present or absent.

Figure 23. The domains of the *vg* ORF that are required to misexpress Sd and rescue *vg* mutant flies are illustrated here. Amino acids 1-170 (red), 279-335 (grey, Sd binding domain) and 336-453 (blue) are necessary to successfully accomplish these two tasks.

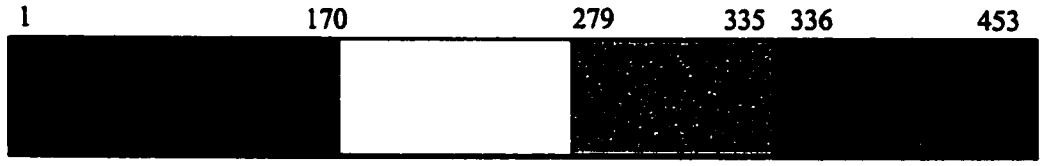
1
170
279
335
336
453

Discussion

Ability of retained regions within *vg* ORF to misexpress Sd

The ability of particular regions of the *vg* ORF to successfully misexpress *sd* was of great interest as part of this study. The close relationship that *sd* and *vg* share to accomplish their respective roles underlies the need to answer this question. It is known that Sd is required for the nuclear localization of Vg (Halder et al., 1998; Simmonds et al., 1998). Therefore, for Vg to act as a nuclear protein and continue its job of effecting other target genes, Sd is needed to ensure that Vg enters the nucleus and can function properly. It has also been shown that in *sd* mutants the ability of Vg to ectopically induce wing tissue (Halder et al., 1998; Simmonds et al., 1998) is hindered. This, again, suggests the necessary cooperation of both Sd and Vg in wing formation. Recent studies were able to show a physical interaction between these two proteins (Simmonds et al., 1998) and specifically the region within Vg that interacts with and binds to Sd (amino acids 279-335). These pieces of information provide further evidence of the requirement for both of these proteins in proper wing formation.

The idea that Vg and Sd act as a transcriptional activator complex for downstream target genes in wing development has been addressed as well. In this scenario, Sd provides the DNA binding activity and the activation domain is contributed by Vg. So, not only is Sd necessary to associate with Vg to allow entrance to the nucleus, but it also is able to then bind specific targets and allow Vg to regulate further gene expression and hence development of the wing. The action of the Vg/Sd complex has been hypothesized to provide selector function in the control of regulatory elements. In

combination with signal transducers, tissue specific responses by these elements can be induced in appropriate areas. Specifically, it is suggested that this type of mechanism is used to induce *cut* (Simmonds et al., 1998), *sal*, *SRF*, *vg*BE, and *vg*QE exclusively in the developing wing pouch (Halder et al., 1998). This specificity needs to be achieved, as there are active signaling pathways for these elements in other tissues. In this way, the Vg/Sd complex functions to restrict their expression to the wing pouch, in parallel with the induction and response to respective signals. For example, the *vg*BE is activated via *Su(H)* in the Notch pathway and is also patterned by the action of Ser and the Vg/Sd complex (see **Figure 7** for model). In this way, the Vg/Sd complex is able to exert effects to regulate target genes and confine expression to the wing disc pouch. Notably, an autoregulatory function is present, as the *vg*BE and *vg*QE are influenced (Halder et al., 1998; Simmonds et al., 1998). These very important qualities have been addressed, in part, in the first section of the work presented here by assessing the misexpression of Sd, via the UAS-Gal4 system (Brand and Perrimon, 1993). It was already known that ectopic expression of *vg* induces the ectopic misexpression of *sd* in the same pattern (Simmonds et al., 1998).

In the results obtained here, it can be discerned that certain portions of the *vg* ORF are necessary to accomplish Sd misexpression. Firstly, the Sd binding domain (amino acids 278-335) must be present. Secondly, it is evident that other portions can be deleted without effect, and some seem to be required. More specifically, amino acids 1-170 and amino acids 336-453 seem to provide an important and redundant role. For example, in deletion Δ5-5, deleting amino acids 2-65, the misexpression ability is slightly reduced, compared to that seen in the full length *vg* construct (**Figure 17 B**). However, in deletion

Δ5-6 and Δ5-7, where larger deletions are made (amino acids 2-170 and 2-278, respectively) the ability to misexpress *sd* is extremely weak (**Figure 17C, D**, respectively). The Δ7-8 construct deletes only amino acids 187-278 and results in a full length *vg*-like ability to misexpress Sd. In deletions Δ1-4 and Δ1-2, which delete amino acids 356-453 and amino acids 335-426, respectively, the misexpression is better than Δ5-5, Δ5-6 and Δ5-7, but not as intense as the full length *vg*. In each of these situations, the deleted regions of one retain the part deleted in the other. For example, in Δ5-6, amino acids 336-453, are intact, whereas in Δ1-4, amino acids 1-277 are intact. Taken together, these data suggest the presence of two important domains in the regions of amino acids 1-170 and amino acids 336-453 for maintaining the ability to ectopically induce Sd. It does seem that there is evidence of a redundant role for these two domains. For example, when amino acids of domain two (amino acids 336-453) are deleted there is still detectable misexpression activity. This is seen in deletions Δ1-4 and Δ1-2, which delete amino acids 356-453 and amino acids 335-426, respectively. The reverse situation is also true. When domain one (amino acids 1-65) is disrupted, there is also still misexpression activity. This activity is notably weaker, as seen in deletions Δ5-5, Δ5-6 and Δ5-7, which delete amino acids 2-65, 2-170 and 2-278, respectively. Together, these data suggest the presence of two activation domains, with the more potent of the two being contained in amino acids 1-170. Deleting regions within this first domain have a more severe effect on misexpression than deleting amino acids of domain two, as seen in the results previously described.

Ability of retained regions within the *vg* ORF to rescue *vg* mutants

To further investigate the necessary portions within the *vg* ORF, the ability of the deleted constructs to successfully rescue two *vg* mutants, vg^{83b27} and vg^{1}, was assessed. This was accomplished by again using the UAS-Gal4 system (Brand and Perrimon, 1993). In these experiments *vg*Gal4;*vg* (vg^{83b27} or vg^{1}) was used to drive UASΔ*vg* expression in a vg^{83b27} or vg^{1} background. Both of these *vg* alleles when homozygous produce a strong *vg* phenotype, and any increase in the amount of wing tissue can be directly attributed to the amount of function retained by the various UAS*vg* constructs.

Similar results were obtained to those of the misexpression assays. All deletion constructs that were able to rescue vg^{83b27} mutants were also able to rescue vg^{1} mutants, and these same constructs retained the ability to ectopically induce *sd*. The same constructs that gave weak misexpression ability (Δ5-5, Δ5-6 and Δ5-7) gave a less complete rescue of the wing. These deletions removed amino acids 2-65, 2-170 and 2-278, respectively. The other deletions that were able to successfully misexpress *sd* correlated with ones able to rescue the vg^{83b27} and vg^{1} mutants. Deletions Δ7-8 (amino acids 187-278 deleted), Δ1-2 (amino acids 335-426 deleted), and Δ1-4 (amino acids 356-453 deleted) are examples of such constructs. The full length *vg* construct did not completely rescue either mutant, and thus, provided a baseline for maximal rescue expectations (**Figure 21A** and **Figure 22A**). There are several possible reasons for the inability of full length *vg* to exhibit a complete rescue. The first explanation concerns the construction of the *vg*Gal4 line that was used in these experiments. It was obtained from Morimura and Hoffmann (unpublished) and was made as follows: the *vg* gene intron 2 region (Williams et al., 1991, 1994) was excised from psub26 (provided by S. Carroll) as

a *Bgl* II- *Bam*HI fragment and cloned into the *Bam*HI site of pGawB (Brand and Perrimon, 1993). Thus, because only the *vg* intron 2 region was used, it might not provide opportunity to give complete rescue. It would provide vgBE activity, but not vgQE activity. Secondly, the chromosomal insertion position of each deletion is arbitrary and therefore could result in a placement close to silencers. This could, in turn, inhibit their acting at full capacity and rescue would be incomplete. Thirdly, crowding effects may have been present that resulted in reduced wing size of the flies resulting in the cross. Finally, the addition of the two extra amino acids, introduced as a result of the *Spe*I used in construction, may be influencing rescue ability. The ability of Δ7-8 to give comparable rescue to that of full length *vg* suggests that this was not a universal problem. However, a positive influence of these extra two amino acids could well be different at the various deletion junctions in the Vg protein. Although the full length *vg* construct gave a less than perfect wing rescue, taking into consideration the three latter factors and comparing the results of the rescues with deleted constructs, this rescue can be considered as complete as possible.

To reiterate the notion that two important domains exist within the *vg* ORF, one can arrive at the same conclusion as with the misexpression assays. Amino acids 1-170 and amino acids 336-453, seem to be playing a very important role in how *vg* interacts with *sd* and consequently its ability to function properly.

Activation domains within *vg*

The identification of the two hypothetical activation domains correlates quite nicely with recent information that has been gathered in studies on the identification of

the human homologue of Vg, Tondu (Tdu). Information on this novel protein was published by Vaudin et al. (1999) and provides both relevance and explanation for the data stated here. In yeast one hybrid experiments, it was shown that there are two activation domains within Vg, corresponding to amino acids 7-127 and amino acids 357-453 . The serendipity of these two separate identifications of activation domains within the *vg* ORF is strong evidence for the authenticity of these two regions. As well, the redundancy that was seen in the various deletions made in this study can be better understood. When one domain was affected, as in Δ5-6 where domain 1 (amino acids 7-127) was deleted, there was still some residual activity. Now, this can be attributed to activation domain 2, localized to amino acids 357-453. In deletions Δ1-2 and Δ1-4, which delete domain 2, the activity of both misexpression and rescue is not affected as much as deleting domain 1. This would suggest a redundant role of these activation domains, as well as the more prominent activity occurring in domain 1.

We can now expand on our interpretation of the *vg* ORF and postulate how it may interact with Sd as a transcriptional activator. Sd binds Vg at amino acids 279-335 in order to facilitate its entrance into the nucleus. Once this is accomplished the Sd protein can bind appropriate targets and enable Vg to activate and control further gene expression. Vg may accomplish this in one of two ways. First, the two activation domains may both be required to some extent to achieve activation, or each is specific to different targets. In any case further control of downstream targets, such as *cut* (Simmonds et al., 1998). *SRF-A*, and *vg* (Halder et al., 1998) can be regulated in this manner (see **Figure 24** for hypothetical model). The notion that Vg is acting as the TIF for Sd is supported by this model. However, it should be noted that there probably exist

Figure 24 Hypothetical model for the actions of Sd and Vg. Sd and Vg interaction is necessary to localize Vg to the nucleus **(A).** Once this Vg/Sd complex is formed it is able to act on downstream targets (target X), such as *SRF-A*, *cut*, and *vg* itself, to regulate transcription **(B).**

A

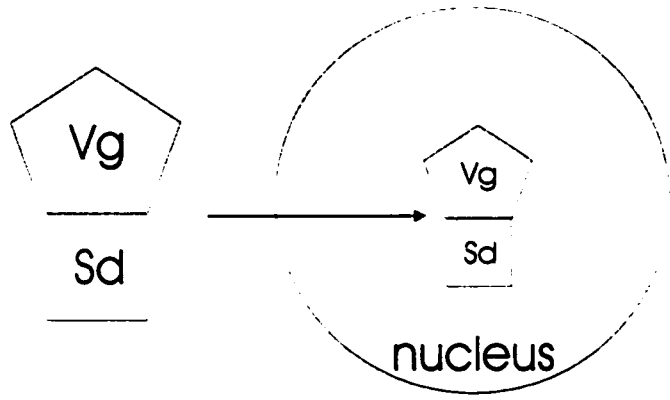

B

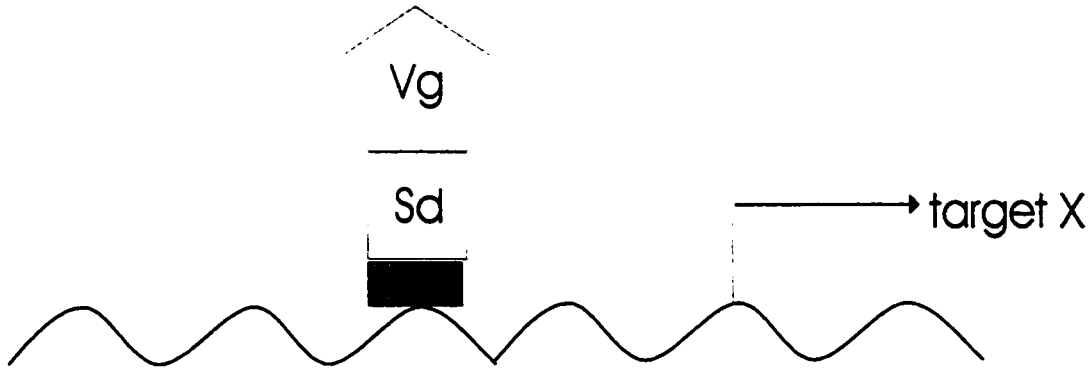

other interacting TIFs for Sd. This is suggested by the requirement of *sd* in other developmental tissues, where *vg* is not expressed (Campbell et al., 1991; Williams et al., 1991). Thus, there are likely other limiting factors for *sd* in these tissues, other than *vg*.

Interpreting activation domains 1 and 2

To examine the sequences of the two activation domains previously described, a BLAST search was done with both the nucleotide and amino acid residues of these regions. There was no significant sequence similarity with any other known transcriptional activators. Thus, rather than examining sequence identity, the amino acid composition was assessed. It has been demonstrated in several studies that activation domains typically have distinct amino acid compositions. For example, the most common residues found are rich in acidic or hydroxylated amino acids (serine, threonine, tyrosine), prolines, glutamines (for reviews see Johnson and McKnight, 1989; Mitchell and Tjian, 1989; Ptashne and Gann, 1990; Carey, 1991) or alanines (Han and Manley, 1993; Huggenvik et al., 1998). The significant amino acid compositions of each domain are as follows: domain one (amino acids 1-170) 13.3% serine, 7.3% glutamine, 5% proline, 18.3% alanine, 5.8% tyrosine, 10.8% glycine, and in domain 2 (amino acids 335-453) 8.3% serine, 18.8% alanine, 8.3% glutamine, 8.3% tyrosine and 15.6% histidine. The amino acid make-up of these two regions is illustrated in **Figure 25**.

Taking this information into consideration, some plausible explanations can be presented. In each case, the highest percent of amino acids was that of alanine. It has been shown that developmental transcription factors often contain alanine-rich regions (Huggenvik et al., 1998). A nuclear DEAF-1-related protein has been identified from

Figure 25. The amino acid compositions of activation domains one **(A)** and two **(B).** Amino acids 7-127 comprise activation domain one, which is rich in alanine (A), serine (S), glycine (G), and tyrosine (Y). The composition of domain two (amino acid 357-453) is comprised of histidine (H), alanine (A), and tyrosine (Y) residues.

Activation domain 1: amino acids 7-127

EVMYGAYYPYLYGRAGTSRRFYQYERFNQDLYPSTGVNLAASSSASGSSH
SPCSPILPPSVSANAAAAVAAAAHNSAAAAVAVAANQASSSGGIGGGGLGG

Activation domain 2: amino acids 357-453

PWVPHAAHYGSYAHAAHAHAAHHAHAYHHNMAQYHSLLRLPQQYASHGSR
LHHDQQTAHALEYSSYPTMAGLEAQVAQVAESSKDLYWFstop

monkey kidney cDNA that has sequence similarity to the *Drosophila* Deformed epidermal autoregulatory factor-1 (DEAF-1) (Huggenvik et al., 1998). These proteins are thought to activate transcription independent of promoter binding. Rather, through protein-protein interactions with basal transcription factors, or other secondary factors, these alanine-rich regions may positively effect transcription. Hypothetically, if the activation domains identified in the *vg*ORF are acting like these alanine-rich transcriptional activators, it could be doing so through protein-protein interactions and controlling downstream targets in this manner. The other notable amino acid contents are that of serine and glutamine, which would correlate with the notion of other transcriptional regulators found to contain high contents of each of these. For example, human Sp1, is a ubiquitously expressed protein that is localized exclusively to the nucleus and contains a glutamine-rich transcriptional activation domain (Courey et al., 1989). The human homologue of *sd*, TEF-1 has both a DNA-binding and activation function. The TEF-1 trans-activation function spans three areas, one of which is rich in hydroxylated amino acids, namely threonine, and interestingly, tyrosine, and serine. This activation domain is considered to have specificity for specific TIFs, which complete the transcriptional activation complex. Because the Vg/Sd complex is thought to carry out the same role as TEF-1, this similarity is quite striking. Another notable piece of evidence known about the activation domains of TEF-1 is that they act cooperatively to achieve their goal. Thus, they are not independent functional transcriptional activators, but rather are constituents of a single activation domain (Hwang et al., 1993).

The other high content residues (glycine in amino acids 7-127 and histidine in amino acids 357-453) do not correlate with any known activation functions. In fact, this

could be indicative of a role for *vg* other than post-transcriptional acivation. Glycine-rich proteins are common in protein kinases that are nucleotide binding proteins (Bossemeyer, 1994) and histidine-rich residues have been implicated in mediating the interaction of transcription factors (Janknecht et al., 1991). Recall that Vg acts in concert with Sd, as do their human counterparts, TEF-1 and TIF. As TEF-1 is limited by its specific TIF, so it is thought that Vg limits Sd function. Therefore, *vg* may perform two separate functions, one to limit or regulate Sd function and one to regulate activated transcription. The idea that Vg and Sd act as a complex is supported, where Sd provides the DNA binding ability and Vg provides activation. However, the story may not end there. There may be subsequent roles wherein Vg influences Sd, in addition to post transcriptional regulation.

Another interesting characteristic of these activation domains suggests interaction with the *Drifter* POU transcription factor. Together, *Mad* and the *Drifter* POU transcription factor act to restrict *vg* expression in the wing imaginal disc (Certel et al., 2000). Interestingly, alanine, glycine, proline and histidine repeats have been found in this evolutionarily conserved family of POU transcription factor genes (Sumiyama et al., 1996).

The similarity between the *D. melanogaster*, *D. virilis* and mosquito *vg* genes has also been assessed previously (Williams et al., 1991). More recently Simmonds et al. (1998) noted that the conserved regions include that identified for Sd binding (amino acids 279-335). Strong conservation is also present in intron 2. This is significant, because the vg^{83b27} mutant is due to a deletion in this region, which encompasses the *vg*BE. It is suspected that a control element in this region is lost (i.e. in vg^{83b27} mutants),

that in other *vg* mutants is not. This provides a possible reason for why vg^{83b27} is able to complement several *vg* alleles (Williams et al., 1991). Upon analysis of the areas identified as activation domains (this study and Vaudin et al., 1999), there is also conservation in these regions between *D. melanogaster*, mosquito and *D. virilis* (Williams et al., 1991).

Comparison of ability to rescue vg^{83b27} and vg^{1}

There were obvious differences observed between vg^{83b27} and vg^{1} in the ability to be rescued. In all deletion constructs that were able to provide any level of rescue of the wing mutations in vg^{1} (full length, Δ5-5, Δ5-6, Δ5-7, Δ7-8, Δ1-2, and Δ1-4), their ability to give some extent of rescue, as assayed by comparisons to the mutant vg^{1} phenotype, was still present, but was not as extensive as in vg^{83b27} rescue. Recalling that vg^{1} is the result of a 412 insertion and vg^{83b27} is a 3kb intronic deletion, that includes the vgBE, it would seem likely that rescuing a mutant that is simply missing portions of the gene (i.e. vg^{83b27}) would be more effective than attempting to rescue a mutant that has additional elements (i.e. vg^{1}). Also, vg^{83b27} can complement other *vg* alleles, perhaps by a transvection-related phenomenon (Williams et al., 1991). This result may offer some explanation about the type of mutation that is occurring in the vg^{1} mutant. If the ability to rescue these mutants is hindered, the 412 insertion that causes the vg^{1} phenotype may be effecting the activation domains of *vg* (or some important functional property of *vg*).

The transposable element 412 in *Drosophila* has been sequenced and shown to contain a eukaryotic viral aspartyl protease active site. The retrotransposon consists of two long ORFs, a long putative leader region, and long terminal repeats (Yuki et al.,

1986). ORF 2 is similar in general organization of the pol gene of Moloney murine leukaemia virus (MoMLV) and codes for the protease, reverse transcriptase and integrase components of the transposable element (Yuki et al., 1986). The long terminal repeats are composed of U3, R, and U5. Although the composition of the 412 insertion is known, the consequences of its insertion are not well understood.

The 412 insertion into the third intron of *vg* results in the production of two transcripts. one wildtype 3.8 kb fragment. and one 3 kb fragment. The second of the two fragments occurs in greater amounts than the first. Thus. the 412 insertion results in the predominant formation of a truncated *vg* transcript (Zider et al., 1996). Further assessment of this truncated product reveals the removal of one of the paired domains of *vg* (Williams et al., 1991). These paired repeats have been identified in other developmental genes. including *paired* and *bicoid* (Frigerio et al., 1986), *daughterless* (Cronmiller et al., 1988), *Deformed* (Regulski et al., 1987) and *E74* (Burtis et al., 1990). While the function of this motif is unknown it has been speculated that it mediates protein-protein interactions that are necessary for transcription factors (Zider et al., 1996). The paired domains are located in amino acids 157-177 and 218-225 and thus do not correlate with the activation domains (amino acids 1-170 and 335-453). This may be indicative of an activity for *vg*, aside from its function in the Vg/Sd complex.

In order to propose reasons for the weaker rescue ability of the *vg* deletion constructs for the vg^{1} mutants, many things have to be taken into consideration. First, as already stated, intuitively one would suspect that rescuing an insertion mutant (vg^{1}) would be more difficult than rescuing a deletion mutant (vg^{83b27}) simply due to the possible hazardous effects introduced by the insert. For example, the vg^{1} mutant exhibits reduced

amount of wildtype *vg* transcript and a high level of a truncated transcript. This could lead to reasons for hindered rescue ability. If this truncated product is disabling the function of Vg in the Vg/Sd complex. this may interfere with other aspects of development that are not rectifiable by introducing deleted fragments of the *vg* ORF. As well, there may be interference between the UASΔ*vg* and the truncated *vg*. Negative or inhibitory effects may be occurring that the UASΔ*vg* constructs are unable to remedy. It is also important to take into account other functions of *vg*. It has been implicated in cell proliferation roles (Zider et al.. 1996), slowed development and reduced viability in mutants (Bazin et al., 1993). These additional effects *vg* exhibits could consequently damage vg^{1} mutants in ways that the UASΔ*vg* constructs are unable to correct. Thus, these deletions may be removing crucial regions necessary for *vg* function in development in general. The introduction of this transposable element into *vg* is probably not only disrupting crucial parts of this gene. but may also consequently be interfering with its ability to interact with other necessary targets (i.e. Dfr, Mad,). Alternatively, vg^{83b27} may be easier to rescue because of the other behaviors it exhibits, such as ability to complement other *vg* alleles.

Future directions

Further dissection of the *vg* ORF is now being done to make a deletion that removes all of the *vg* ORF except the Sd binding domain (amino acids 278-335). This region has already been shown to be necessary and sufficient for binding of Sd and TEF-1 (Simmonds et al., 1998). This will conclusively prove that without the activation domains no misexpression or rescue can occur. Its construction is similar to all other

constructs: inverse PCR in pUC19 and subcloning of the deletion into pUAST. Deletion construct Δ1-4 deletes amino acids 356-453, therefore, by using this is as a template in PCR reactions with primers 5 and 7, amino acids 2-278 will also be deleted. Hence, the final product will leave only amino acids 279-335 intact. This will include the desired region (Sd binding domain, amino acids 279-335) and exclude the two activation domains (amino acids 1-170 and 336-453). This construct is being made in preparation for micro-injections. Since there is a functional redundancy in Vg for activation, the removal of only one domain does not completely destroy the ability of Vg to execute its function. However, it is a clear prediction that if only the portion of Vg that provides the ability to bind Sd is retained, there can be no ability to ectopically induce *sd*, nor to rescue a *vg* mutant allele.

References

Ashburner, M., and T.R.F. Wright. 1978. The genetics and biology of *Drosophila*. Academic Press p. 108-113, 230-247.

Asburner, M. 1989. Drosophila: A laboratory handbook. Cold Spring Harbor Laboratory Press.

Bazin, C., J.A. Williams, J. Bell, and J. Silber. 1993. A deleted *hobo* element is involved in the thermosensitive unstable vg^{al} mutation at the *vestigial* locus *in D. melanogaster*. Genetical Research 61: 171-176.

Bossemeyer, D. 1994. the glycine-rich sequence of protein kinases: a multifunctional element. Trends in Biochemical Sciences. 19: 201-205.

Bownes, M., and S. Roberts. 1981. Regulative properties of wing discs from the *vestigial* mutant of *Drosophila melanogaster*. Differentiation 18: 89-96.

Brand, A.H., and N. Perrimon. 1993. Targeted gene expression as a means of altering cell fates and generating dominant phenotypes. Development 118: 401-415.

Brunk, B.P., E.C. Martin, and P.N. Adler. 1991. *Drosophila* genes *Posterior Sex Combs* and *Suppressor two of zeste* encode proteins with homology to the murine *bmi-1* oncogene. Nature 353: 351-353.

Bryant, P.J. 1975. Pattern formation in the imaginal wing disc *of Drosophila melanogaster*: fate map, regeneration and duplication. Journal of Experimental Zoology 193: 49-78.

Burtis, K.C., C.S. Thummel, C. Weldon Jones, F.D. Karim, and D.S. Hogness. 1990. The *Drosophila* 74EF early puff contains *E74*, a complex ecdysone-inducible gene that encodes two *ets*-related proteins. Cell 61: 85-99.

Campbell, S.D., A. Duttaroy, A.L. Katzen, and A. Chovnick. 1991. Cloning and characterization of the *scalloped* region of *Drosophila melanogaster*. Genetics 127: 367-380.

Campbell, S., M. Inamdar, V. Rodrigues, V. Raghavan, M. Palazzolo, and A. Chovnick. 1992. The *scalloped* gene encodes a novel, evolutionarily conserved transcription factor required for sensory organ differentiation in *Drosophila*. Genes and Development 6: 367-379.

Campbell,G., and A. Tomlinson. 1999. Transducing the Dpp morphogen gradient in the wing of Drosophila: regulation of Dpp targets by brinker. Cell 96: 553-562.

Campos-Ortega, J.A., and V. Hartenstein. 1985. The embryonic development of *Drosophila melanogaster*. Springer Berlag, Berlin.

Carey. M. 1991. Mechanistic advances in eukaryotic gene activation. Current Opinion in Cell Biology 3: 452-460.

Casares. F.. and R.S. Mann. 2000. A dual role for *homothroax* in inhibiting wing blade development and specifying wing identities in *Drosophila*. Development 127: 1499-1508.

Certel K.. A. Hudson. S.B. Carroll. and W.A. Johnson. 2000. Restricted patterning of vestigial expression in Drosophila wing imaginal discs requires synergistic activation by both Mad and the Drifter POU domain transcription factor. Development 127: 3173-3183.

Courey. A.J.. D.A. Holtzman. S.P. Jackson. and R. Tjian. 1989. Synergistic Activation by the Glutamine-rich domains of Human Transcription Factor Sp1. Cell 59: 827-836.

Crick, F.H.C., and P.A. Lawrence. 1975. Compartment and polyclones in insect development. Science 189: 340-347.

Cronmiller. C.. P. Schekl. and T.W. Cline. 1988. Molecular characterization of *daughterless*. a *Drosophila* sex determination gene with multiple roles in development. Genes and Development 2: 1666-1676.

Deshpande. N., A. Chopra. A. Rangarajan. L.S. Shashidhara. V. Rodrigues. S. Krishna. 1997. The human transcription enhancer factor-1. TEF-1. can substitute for Drosophila scalloped during wingblade development. Journal of Biological Chemistry 16:10664-10668.

Foe. B.E.. and B.M. Alberts. 1983. Studies of nuclear and cytoplasmic behaviours during the five mitotic cycles that precede gastrulation in *Drosophila* embryogenesis. Journal of Cell Science 61: 31-70.

French, V., P.J. Bryant, and S.V. Bryant. 1976. Pattern regulation in epimorphic fields. Science 193: 969-981.

Frigerio, G., M. Burri, D. Bopp. S. Baumgartner, and M. Noll. 1986. Structure of the segmentation gene *paired* and the *Drosophila PRD* gene set as part of a gene network. Cell 47: 2188-2201.

Fristrom. D. 1969. Cellular degeneration in the production of some mutant phenotypes of *Drosophila melanogaster*. Molecular and General Genetics 103: 363-391.

Garcia Bellido, A., P. Ripoll, and G. Morata. 1976. Developmental compartmentalization in the dorsal mesothoracic disc of *Drosophila*. Developmental Biology 48: 132-147.
Goldstein, L.S.B., and E.A. Fyrberg. 1994. *Drosophila melanogaster*: Practical Uses in Cell and Molecular Biology. Academic Press.

Gowen, J.W., and L.E. Johnson. 1946. On the mechanism of heterosis I. Metabolic capacity of different races of *Drosophila melanogaster* for egg production. American Naturalist. 80: 149-179.

Halder, G., P. Polaczyk, M.E. Kraus, A. Hudson, J. Kim, A. Laughon, and S. Carroll. 1998. The Vestigial and Scalloped proteins act together to directly regulate wing-specific gene expression in *Drosophila*. Genes and Development 12: 3900-3909.

Han, K., and J.L. Manley. 1993. Functional domains of the Drosophila Engrailed protein. EMBO Journal 12: 2723-2733.

Huggenvik, J.I., R.J. Michelson, M.W. Collard, A.J. Ziemba, P. Gurley, and K.A. Mowen. 1998. Characterization of a nuclear deformed epidermal autoregulatory factor-1 (DEAF-1)-related (NUDR) transcriptional regulator protein. Molecular Endocrinology 12: 1619-1639.

Hwang, J.J., P. Chambon, and I. Davidson. 1993. Characterization of the transcription activation function and the DNA binding domain of transcriptional enhancer factor-1. EMBO Journal 6: 2337-2348.

Ingham, P.W. 1988. The molecular genetics of embryonic pattern formation in *Drosophila*. Nature 335: 25-34.

Inoue, H., H. Nojima, and H. Okayama. 1990. High efficiency transformation of *Escherichia coli* with plasmids. Gene 96: 23-28.

Jacquemin, P., J. Hwang, J.A. Martial, P. Dolle, and I. Davidson. 1996. A novel family of developmentally regulated mammalian transcription factors containing the TEA/ATTS DNA binding domain. Journal of Biological Chemistry. 271:21775-85.

Janknecht, R., C. Sander, and O. Pongs. 1991. (HX)n repeats: a pH-controlled protein-protein interaction motif of eukaryotic transcription factors? FEBS Letters 295: 1-2.

Jazwinska, A., C. Rushlow, and S. Roth. 1999a. The role of *brinker* in mediating the graded response to Dpp in early *Drosophila* embryos. Development 126: 3323-3334.

Jazwinska A., N. Kirov, E. Wieschaus, S. Roth, and C. Rushlow. 1999b. The *Drosophila* gene *brinker* reveals a novel mechanism of Dpp target gene regulation. Cell 96: 563-573.

Johnson, P.F., and S.L. McKnight. 1989. Eukaryotic transcriptional regulatory proteins. Annuual Review Biochemistry 58: 799-839.

Kelly, J.J., and A.G. Wildeman. 1991. Role of the SV40 enhancer in the early to late shift in viral transcription. Nucleic Acids Research. 19: 6799-6804.

Kim, J., A. Sebring, J.J. Esch, M.E. Kruas, K. Vorwerk, j.Magee, and S.B. Carroll. 1996. Integration of positional signals and regulation of wing formation and identity by *Drosophila vestigial* gene. Nature 382: 133-138.

Klein, T., and A.M. Arias. 1999. The Vestigial gene product provides a molecular context for the interpretation of signals during the development of the wing in *Drosophila*. Development 126: 913-925.

Mitchell, P.J., and R. Tjian. 1989. Transcriptional regulation in mammalian cells by sequence-specific DNA binding proteins. Science 245: 371-378.

Morgan. T.H. 1911. The origin of nine wing mutations in *Drosophila*. Science 33: 496-498.

Nakashima-Tanaka E. 1967. The effect of temperature and genetic background on the phenotypic expression of several *vestigial* strains of *Drosophila melanogaster*. Genetica 38: 447-458.

Neumann. C.J., and S.M.Cohen. 1997. Long-range action of Wingless organizes the dorsal-ventral axis of the *Drosophila* wing. Development 124: 871-880.

Nojima. I.H., and H. Okayama. 1990. High efficiency transformation of *Escherichia coli* with plasmids. Gene 96: 23-28.

Nusslein-Volhard, C. and R. Wieschaus. 1980. Mutations affecting segment number and polarity in *Drosophila*. Nature 281: 795-801.

Nusslein-Volhard, C., H.G. Frohnhofer, R. Lehmann. 1987. Determination of anteroposterior polarity in *Drosophila*. Science 238: 1675-1681.

Paumard-Rigal S., A. Zider, P. Vaudin, and J. Silber. 1998. Specific interactions between *vestigial* and *scalloped* are required to promote wing tissue proliferation *in Drosophila melanogaster*. Development Genes and Evolution 208: 440-446.

Peifer, M., F. Karch, and W. Bender. 1987. The bithorax complex: control of segmental identity. Genes and Development 1: 891-898.

Ptashne. M., and A.A.F. Gann. 1990. Activators and targets. Nature 335: 563-565.

Regulski, M., N. McGinnis, R. Chadwick, and W. McGinnis. 1987. Developmental and molecular analysis of *Deformed*; a homeotic gene controlling *Drosophila* head development. EMBO Journal 6: 767-777.

Shapiro, H. 1932. The rate of oviposition in the fruit fly, Drosophila. Biological Bulletin (Woods Hole) 63: 456-471.

Simmonds. 1997. The developmental effects of dominant *invected* and *vestigial* mutations in Drosophila melanogaster. PhD thesis.

Simmonds, A.J., X. Liu, K.H. Soanes, H.M. Krause, K.D. Irvine, and J.B. Bell. 1998. Molecular interactions between Vestigial and Scalloped promote wing formation in *Drosophila*. Genes and Development 12: 3815-3820.

Stanley, W. 1931. The effect of temperature on *vestigial* wing in *Drosophila melanogaster*, with temperature effective periods. Physiological Zoology IV: 394-408.

Sumiyama, K., K. Washio-Watanabe, N. Saitou, T. Hayakawa, and S. Ueda. 1996. Class III POU genes: generation of homopolymeric amino acid repeats under GC pressure in mammals. Journal of Molecular Evolution 43: 170-178.

Varadarajan, S., and K. VijayRaghavan. 1999. *scalloped* functions in a regulatory loop with *vestigial* and *wingless* to pattern the *Drosophila* wing. Development Genes and Evolution 209: 10-17.

Vaudin, P., R. Delanoue, I. Davidson, J. Silber, and A. Zider. 1999. TONDU (TDU), a novel human protein related to the product of *vestigial* (*vg*) gene of *Drosophila melanogaster* interacts with vertebrate TEF factors and substitutes for Vg function in wing formation. Development 126: 4807-4816.

Vieira, J. and J. Messing. 1982. The pUC plasmids, an M13mp7-derived system for insertion mutagenesis and sequencing with synthetic universal primers. Gene 19: 259-268.

Williams J.A., and J.B. Bell. 1988. Molecular organization of the vestigial region in Drosophila melanogaster. EMBO Journal 7: 1355-1363.

Williams J.A., I.M. Scott, A.L. Atkin, W.J. Brook, M.A. Russell, and J.B. Bell. 1990. Genetic and molecular analysis of vg^{U} and vg^{W}: two dominant *vg* alleles associated with gene fusions in Drosophila. Genetics 125: 833-844.

Williams J.A., J.B. Bell, and S.B. Carroll. 1991. Control of *Drosophila* wing and haltere development by the nuclear *vestigial* gene product. Genes and Development 5: 2481-2495.

Williams, J.A., S.W. Paddock, and S.B. Carroll. 1993. Pattern formation in a secondary field: a hierarchy of regulatory genes subdivides the developing *Drosophila* wing disc into discrete subregions. Development 117: 571-584.

Williams, J.A., S.W. Paddock, K. Vorwerk, and S.B. Carroll. 1994. Organization of wing formation and induction of a wing-patterning gene at the dorsal/ventral compartment boundary. Nature 368: 299-305.

Xiao, J.G., I Davidson, H. Matthes, J. Garnier, and P. Chambon. 1991. Cloning, expression, and transcriptional properties of the human enhancer factor TEF-1. Cell 65: 551-568.

Yuki, S., S. Ishimaru, S. Inouye, and K. Saigo. 1986. Identification of genes for reverse transcriptase-like enzymes in two *Drosophila* retrotransposons, 412 and gypsy: a rapid detection method of reverse transcriptase genes using YXDD box probes. Nucleic Acids Research 14: 3017-3030.

Zecca, M., K. Basler, and G. Struhl. 1996. Direct and long-range action of a *wingless* morphogen gradient. Cell 87: 833-844.

Zider, A., D. Flagiello, I. Frouin, and J. Silber. 1996. *vestigial* gene expression in *Drosophila melanogaster* is modulated by the dTMP pool. Molecular and General Genetics 251: 91-98.